Positive *P* representation: Application and validity

A. Gilchrist, C. W. Gardiner,* and P. D. Drummond†
University of Waikato, Hamilton, New Zealand
(Received 8 July 1996)

The positive *P* representation is a very successful tool in quantum optics. However, the usual assumption of negligible boundary terms in the time-evolution equations is not always valid. We explore the range of validity of the time-evolution equations both analytically and by numerical investigation of a number of specific examples. We present practical ways of verifying the validity of the use of the positive *P* representation and find that the standard time-evolution equation can become invalid when nonlinear terms (at unit photon number) are large relative to the damping rate. This is very much larger than is normally the case in nonlinear optics, except possibly near resonances. We are able to show that when the positive *P* representation is invalid, the boundary terms, normally neglected in an integration by parts, become non-negligible. When numerical simulations are carried out using the positive *P* representation, specific checks given in this paper should be carried out to verify the compactness of the distribution. In conclusion, we find that (apart from special cases) this technique of quantum time evolution is typically asymptotically valid in the limit of small nonlinearity, rather than exact. [S1050-2947(97)01803-9]

PACS number(s): 42.50.Ct, 42.55.−f, 42.65.−k, 42.50.Ar

I. INTRODUCTION

Since the invention more than thirty years ago of the *P* representation by Glauber [1] and Sudarshan [2], much of theoretical quantum optics has been dominated by the applications of this representation, which mimics, but does not precisely duplicate, the classical equations of electromagnetism. The original Glauber-Sudarshan *P* representation is a normally ordered operator representation, most suited to situations in which the behavior of the electromagnetic field is almost classical. Other well-known phase-space representations include the Wigner [3] (symmetrically ordered) and *Q* [4,5] (antinormally ordered) representations. The principal advantage of a normally ordered representation is that the vacuum fluctuations are included in the definition of the representation, and thus a low-temperature situation can be represented almost classically.

All phase-space representations are simply transcriptions of quantum mechanics. Sometimes this transcription yields simple and possibly illuminating results—for example, the master equation for a damped harmonic oscillator is transformed into a classical Fokker-Planck equation, yielding an interpretation of great utility. Sometimes extra noise appears as a result of quantum mechanics, but the interpretation remains qualitatively similar. However, this simple picture does not always pertain. There are two major problems to be dealt with: (i) the Glauber-Sudarshan *P* representation need not always yield the *positive P* function that is required for the interpretation of any Fokker-Planck equation that may be derived as a stochastic equation, and (ii) the Fokker-Planck equations that are derived may include higher than second-order derivatives.

We do not consider the second problem here. It typically does not occur in normally ordered representations with the types of model nonlinear Hamiltonian that are treated here. In other cases, methods have been derived for determining under what conditions such higher-order derivatives may be neglected [6]. In general, with normal-ordered representations, these problems are usually restricted to atomic-operator Hamiltonians, which have non-Bose commutators. However, even in the pure Bose commutator case, higher derivative terms create a prevalent difficulty in treating nonlinear Hamiltonians with representations that are not normally ordered, such as the Wigner or *Q* representations.

The first problem was solved by Drummond and Gardiner [7] by devising the *positive P* representation. This is a generalization of the normally ordered Glauber-Sudarshan *P* representation, in which an initial (nondiagonal) *P* function can always be chosen, which is guaranteed both to exist and to be positive. Provided boundary terms vanish in certain partial integrations, it was shown that a time-dependent positive distribution function could also be chosen to satisfy a Fokker-Planck equation. This occurs in a phase space that has twice the dimension of the classical phase space. The additional dimensions have the simple interpretation that they allow an expansion of the quantum density matrix with off-diagonal coherent state terms.

One of the qualities that makes the positive *P* representation so attractive is that it enables the dynamics of a system to be explored by numerical simulation of *c*-number stochastic differential equations. This allows the full nonlinearities to be included in the analysis. All quantum-mechanical states can be treated without problem, due to the expanded phase space. In contrast, other phase-space techniques for operator representations can rapidly run into problems, for certain quantum states or master equations.

The Glauber-Sudarshan *P* representation does not necessarily exist as a well-behaved positive function (although Klauder and Sudarshan [8] have shown that it does exist in terms of extremely singular distributions). The Wigner function can be negative for some quantum states, which pre-

*Present address: Victoria University, Wellington, New Zealand.
†Present address: University of Queensland, Queensland, Australia.

cludes a probabilistic interpretation. It also typically leads to Fokker-Planck equations with higher than second-order derivatives. This situation is not intractable, and in suitable conditions the higher-order derivatives can be truncated, so that it is possible to arrive at stochastic differential equations [6]. There can obviously be situations where this truncation will lead to inaccuracies when compared with the true solution. Thus, there have been studies where the positive P representation equations agree with the exact quantum solution, even though the truncated Wigner equations do not [9–11]. Finally, the Q function, although positive and normalized, has the disadvantage that not every positive Q function corresponds to a positive semidefinite Hermitian density operator, also the time-evolution equation is usually neither second order nor positive definite. This means that no stochastic interpretation exists in the phase-space sense, so that numerical stochastic treatments are not generally possible.

The positive P distribution has consequently resulted in a very useful technique in quantum optics [9–38], with systems ranging from microdisk lasers [35] to solitons [16,32,37]. It has, for instance, been extensively used in the study of nonclassical light. Topics include antibunching [27], generation of superposition states [28–30], Bell's inequalities [26], and, in particular, the study of squeezing [11,12,16,18–20,22,24,25,32,33]. There has even been an interesting proposal to directly measure the positive P distribution [36].

However, simulations of positive P stochastic equations have not been widely used as a numerical tool in quantum optics. In 1978, when the ideas were first being developed, Steyn [39] attempted such simulations for the problem of a phase-damped anharmonic oscillator, and found that the practical implementation of the method did have some numerical difficulties. The source was not at that time entirely clear. In due course, other workers investigated various problems to which numerical positive P simulations seemed appropriate. It was found that, in practice, once numerical difficulties were dealt with there were two problems left — both related to questions of stability [40–46].

The positive P equations of motion take place with twice as many variables as in the Glauber-Sudarshan P representation. In the Glauber-Sudarshan equations, we would have a complex amplitude α, and its complex conjugate α^*. In the positive P equations, one has two *independent* complex variables α and α^+. Generally, positive P equations of motion can be obtained by the deceptively simple substitution $\alpha^* \rightarrow \alpha^+$ in the Glauber-Sudarshan stochastic differential equations, provided the stochastic terms are chosen correctly.

The dynamical stability in this analytically continued phase space of doubled dimensions is dramatically different from that of the classical phase space [40–42,45]. For instance, limit cycles are turned into two-dimensional manifolds with the diffusion spreading the distribution along the manifold [40,45]. This may eventually cause a problem, since any finite ensemble of points representing a distribution will drift apart. This ensemble may then cease to be a sufficiently fine sampling of the underlying distribution, leading to increased numerical errors. This is essentially a practical problem and may be amenable to more subtle numerical schemes. For instance, Kinsler, Fernée, and Drummond [11] simulate the *difference* between their stochastic process and an appropriately chosen, exactly soluble, stochastic differential equation with similar diffusion. The difference can then be added to the solution of the exact equation to give the required quantity.

More seriously, in some cases where the nonlinearity (at unit photon number) is comparable with the linear decay rate, the positive P representation may simply give the wrong result [43–46]. The issue in this case is the validity of neglecting the boundary terms in the derivation of the dynamical equations. In all cases where these problems occur, they can be traced to the existence of at least one singular trajectory in the deterministic dynamics of the extended phase space. Even if this singularity occurs with zero probability (as is typically the case), the distribution in the neighborhood of this singular trajectory may not vanish sufficiently rapidly at large phase-space radii. This can generate additional terms that are usually neglected in the partial integrations used to derive the dynamical equations.

In all cases of Hamiltonians bilinear in creation and destruction operators, and linear damping, the boundary requirements are trivially satisfied. Thus, for example, the linear harmonic oscillator has no boundary terms, so that the treatment of damping by the Glauber-Sudarshan P representation can easily be extended to cover any nonclassical quantum state. Similarly, linear or linearized equations have no boundary problems; and much of the use of the positive P representation is in this context [12–27]. Finally, if the phase-space dynamics can be confined to a bounded manifold (as in the parametric oscillator with the driving field adiabatically eliminated [9,28–30]), then the boundary terms may not exist.

We emphasize that when boundary-term problems have occurred they invariably have occurred in systems whose nonlinearity parameters were set to values much higher than those of any known physical system. We can define the dimensionless nonlinearity of a system as γ^{-1}, where γ represents the boson occupation number for which the linear decay rate equals the nonlinear rate of change. The smaller the value of γ the more nonlinear the system, and the lower the dimensionless linear damping. Typically, problems have been found for linear damping below a critical value of $\gamma \simeq 1$. Within this parameter regime of high nonlinearity (and very small photon numbers) there are often other methods, such as directly simulating the master equation [47], that are very effective. As the nonlinearity of the system is decreased the positive P representation can quickly become accurate and computationally superior to other methods [9].

There are no known problems with the positive P representation in realistic systems, which generally have $\gamma \geqslant 10^3$. However, larger nonlinearities leading to smaller γ could well occur in future systems in quantum electronics, due to the drive towards reduced cavity size in many experiments; and so clarifying the validity of the positive P representation is important.

It is now timely for a definitive statement to be made on the validity of the positive P representation. This paper will give practical guidelines on how to use the positive P representation correctly and reliably. In particular the aim is to provide numerical signatures that herald an unreliable solution. To this aim we will concentrate on rather unreasonably high nonlinearities and tiny photon numbers—a regime most

unsuitable for the practical use of the positive P representation, but one in which it becomes possible to analyze the origins of unreliable solutions. In Sec. II we present the numerical signatures. Sections III and IV examine various models where the positive P representation fails and demonstrate the usefulness of the numerical signatures, while Sec. V examines a model where the positive P gives correct answers but must be treated with care as far as the numerical signatures are concerned. Section VI presents theoretical arguments supporting the use of these signatures. Lastly, in Appendix A we give an example of a nonlinear stochastic equation that is analytically tractable, and illustrates the relationship of the numerical signatures to the large-radius behavior of the corresponding probability distribution.

II. NUMERICAL SIGNATURES OF BOUNDARY PROBLEMS

We have studied all the models that have appeared in the literature in which the positive P representation gave a false solution [43–46]. These studies of the representation have produced a surprising and powerful result—when the equations fail they do so in a recognizable way, giving rise to certain simple numerical signatures that herald the appearance of finite boundary terms and an unreliable solution.

In the derivation of a positive-P Fokker-Planck equation from a master equation, it is necessary to discard the boundary terms that turn up in the integration by parts. This is an essential part of the whole procedure. If this step is not valid then the dynamics of the Fokker-Planck equation will not be equivalent to that of the quantum system described by the original master equation.

The initial distribution presents no problem, as Drummond and Gardiner [7] gave a prescription for writing an equivalent P function for a given density operator. Provided the time evolution of the Fokker-Planck equation as given by the stochastic differential equations does not explore a boundary at a large distance then it will continue to have solutions equivalent to the solutions from the master equation. The question then becomes: Can the stochastic differential equations explore arbitrarily distant regions in phase space? If this happens, there is a danger that the evolution of the Fokker-Planck or stochastic equations will give different results from the master equation.

In particular, we have found that the following signs indicate that boundary terms are likely to have a significant effect.

(1) The presence of near-singular trajectories, which make large excursions into regions of phase space where α and α^+ are far from being complex conjugate. In particular, the time of the earliest such trajectory in a large ensemble is a good indicator of when the solution develops significant boundary terms. It has been a common practice to remove these trajectories from ensemble averaging [40,48,49], although such a procedure in no way solves the problem. These trajectories (or ''spikes'') give one of the first warning signs to pick up. However, care must be taken that trajectories of this type are not just numerical artifacts due to unstable integration algorithms. In our simulations, we use stable implicit algorithms that are strongly convergent in the stochastic sense. This allows each trajectory to be checked to ensure that it has converged in the limit of small step size.

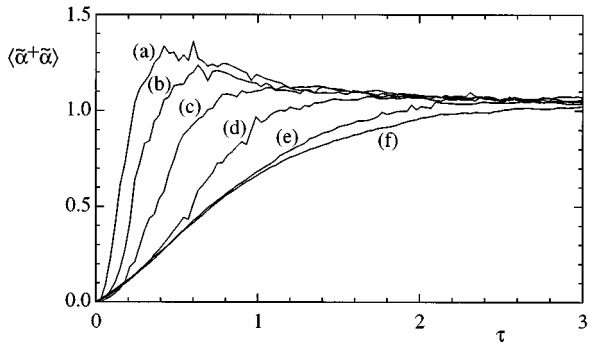

FIG. 1. Mean photon number for the single-mode laser starting from ''equivalent'' initial Gaussian distributions: variance (a) $\sigma^2=1$, (b) $\sigma^2=0.8$, (c) $\sigma^2=0.6$, (d) $\sigma^2=0.4$, (e) $\sigma^2=0.2$, and (f) $\sigma^2=0$.

(2) Another readily monitored warning sign is a sudden increase in the statistical error due to the finite ensemble size. This is useful because, in conjunction with the onset of spiking, there is also a substantially greater variance in any average over the distribution. However, as in the previous signature, this indicator can be misleading, due to its qualitative nature.

(3) If the previous two indicators are present then we recommend a quantitative exploration of the behavior of the distribution at large radius. If the large radius tails of the distribution fall off as a power law—for example, $P(|\alpha^+\alpha|)\simeq|\alpha^+\alpha|^{-n}$—then, if n is too small, there will certainly be significant boundary terms. The value of n that can be considered large enough will depend on the problem being simulated.

(4) Finally, an increase of the linear damping rate in the model being considered will tend to restrict the large excursions of trajectories. In effect, there is a barrier that has to be surmounted by the diffusion. Since this serves to restrict the trajectories to a bounded domain then boundary-term problems should cease as the linear damping rate is increased.

If all these signatures occur simultaneously, it is highly likely that boundary terms are becoming significant. This means the solutions given by the stochastic equations are no longer equivalent to the solutions of the master equation.

We now examine several models where the positive P method yields an incorrect solution and in each model we present the various numerical indices described above together with any analytical work possible.

III. THE SINGLE-MODE LASER

In a recent publication Schack and Schenzle [46] claimed that for the positive P model of the single-mode laser, the vacuum initial condition, when represented by

$$P(\alpha,\alpha^+,t=0)=\delta(\alpha)\,\delta(\alpha^+), \tag{3.1}$$

gives the correct results depicted in Fig. 1 curve (f), but that the choice of initial distribution corresponding to that given by Drummond and Gardiner [7],

$$P(\alpha,\alpha^+,t=0)=\frac{1}{4\pi^2}\exp\left(-\frac{|\alpha-\alpha^+|^2}{4}\right)\times\left\langle\frac{\alpha+\alpha^+}{2}\middle|0\right\rangle\left\langle0\middle|\frac{\alpha+\alpha^+}{2}\right\rangle=\frac{1}{4\pi^2}\exp\left\{-\frac{1}{2}(|\tilde{\alpha}|^2+|\tilde{\alpha}^+|^2)\right\} \quad (3.2)$$

gave different results, depicted in curve (a) of Fig. 1. This choice is of interest because any quantum state can be represented in this form, even though there are often simpler choices available in any particular case—such as the vacuum state, which also has a delta-function representation. We will show that Schack and Schenzle did not treat this distribution consistently, and that their anomaly does not occur for any practical values of parameters. In other words, even the model itself is questionable when using their approximate laser equation, with parameters that result in the above anomaly. Nevertheless, we can draw some interesting conclusions from their work.

We start from the *unscaled* Fokker-Planck equation for the single mode laser [50],

$$\frac{\partial P(\alpha,\alpha^+)}{\partial t}=\left\{\frac{\partial}{\partial\alpha}\left[\kappa\alpha\left(1-\frac{C}{1+\alpha^+\alpha/n_0}\right)\right]+\frac{\partial}{\partial\alpha^+}\left[\kappa\alpha^+\left(1-\frac{C}{1+\alpha^+\alpha/n_0}\right)\right]+\left[2\kappa n+\mathcal{N}(1+\overline{d})\frac{\overline{g}^2}{\overline{\gamma}}\right]\frac{\partial^2}{\partial\alpha\partial\alpha^+}\right\}P(\alpha,\alpha^+), \quad (3.3)$$

where $\mathcal{N}$ is the number of atoms, C is the cooperativity parameter, which determines the behavior of the laser, and n_0 is the saturation photon number. $\overline{\gamma}$, $\overline{d}$, and g are parameters. It is important to note that in the derivation of this equation several assumptions were made and hence the equation does not correspond exactly to a master equation. Despite this, the mechanism by which the positive P representation breaks down here appears to be generic.

Now, in order to simplify Eq. (3.3) we introduce the *scaled* quantities $\tilde{g}$, $\tilde{n}_0$, $\tilde{\alpha}$, and $\tilde{q}$ defined by

$$g=\tilde{g}/\sqrt{\mathcal{N}}, \quad (3.4a)$$

$$n_0=\tilde{n}_0\mathcal{N}=\overline{\gamma}^2\mathcal{N}/(2\tilde{g}^2), \quad (3.4b)$$

$$\alpha=\tilde{\alpha}\sqrt{\mathcal{N}}, \quad (3.4c)$$

$$\tilde{q}=[\kappa n/\mathcal{N}+\tilde{g}^2(1+\overline{d})/(2\overline{\gamma}\mathcal{N})]. \quad (3.4d)$$

Finally, since for the validity of the choice of the form of $\tilde{q}$ it was assumed that $\tilde{\alpha}^+\tilde{\alpha}\ll\tilde{n}_0$, we can again make use of this assumption to invoke a binomial expansion to first order to arrive at the rotating-wave van der Pol laser equation

$$\frac{\partial P(\tilde{\alpha},\tilde{\alpha}^+)}{\partial t}=\left\{-\frac{\partial}{\partial\tilde{\alpha}}\left[\kappa(C-1)\tilde{\alpha}-\frac{\kappa C\tilde{\alpha}^+\tilde{\alpha}^2}{\tilde{n}_0}\right]-\frac{\partial}{\partial\tilde{\alpha}^+}\left[\kappa(C-1)\tilde{\alpha}^+-\frac{\kappa C\tilde{\alpha}^{+2}\tilde{\alpha}}{\tilde{n}_0}\right]+2\tilde{q}\frac{\partial^2}{\partial\tilde{\alpha}\partial\tilde{\alpha}^+}\right\}P(\tilde{\alpha},\tilde{\alpha}^+). \quad (3.5)$$

From this we can write the Ito stochastic differential equations [51]

$$d\tilde{\alpha}=(\epsilon\tilde{\alpha}-\tilde{\alpha}^+\tilde{\alpha}^2)d\tau+\sqrt{\tilde{Q}}dW, \quad (3.6a)$$

$$d\tilde{\alpha}^+=(\epsilon\tilde{\alpha}^+-\tilde{\alpha}^{+2}\tilde{\alpha})d\tau+\sqrt{\tilde{Q}}dW^*, \quad (3.6b)$$

where time has been scaled by setting $dt=d\tau\,\tilde{n}_0/\kappa C$ with $\tilde{q}=\tilde{Q}\kappa C/\tilde{n}_0$ and $\epsilon=\tilde{n}_0(C-1)/C$. The noise $dW=dW_1+i dW_2$ and $\langle dW^*dW\rangle=2d\tau$. Equations (3.6) are the equations as used by Schack and Schenzle [46].

The initial condition in the *scaled* variables (3.4) is

$$P(\tilde{\alpha},\tilde{\alpha}^+,t=0)=\frac{\mathcal{N}^2}{4\pi^2}\exp\left\{-\frac{\mathcal{N}}{2}(|\tilde{\alpha}|^2+|\tilde{\alpha}^+|^2)\right\}, \quad (3.7)$$

whose variance is $\sigma^2=1/\mathcal{N}^2$, which in any practical case is very small. The effect of this scaling was omitted by Schack and Schenzle, so that their conclusions, while interesting, do not invalidate the choice of Eq. (3.2) as an initial distribution. In fact as the variance of the initial distribution as used by Schack and Schenzle is reduced, the results become indistinguishable from those obtained from an initial delta distribution as shown in Fig. (1). One could argue that the laser model could also be applied in the critical region near threshold, which would give a larger value for the initial variance. This is possible, but is accompanied by a great increase in the noise parameter; see Appendix B. This increased noise was also omitted by Schack and Schenzle.

The initial vacuum state can, however, be represented by Gaussian distributions of arbitrary variance [7], so the conclusions of Schack and Schenzle are worthy of study, especially as we shall see that they illuminate the general mechanism of the breakdown of the positive P simulations.

A. Analytic treatment via the deterministic equation

In this section we will demonstrate that the mechanism for the breakdown of the positive P simulations exists even in the deterministic equations alone. To show this we concentrate on the closed equation for the photon number [52] $\tilde{N}=\tilde{\alpha}^+\tilde{\alpha}$,

$$d\tilde{N}=-2(\tilde{N}-a)(\tilde{N}-b)d\tau+2\sqrt{\tilde{Q}\tilde{N}}dW, \quad (3.8)$$

where dW is now a real Wiener increment, with $\langle dW^2\rangle=d\tau$. In the Stratonovich form of the equation, a and b are given by

$$\left.\begin{matrix}b\\a\end{matrix}\right\}=\frac{\epsilon}{2}\pm\sqrt{\left(\frac{\epsilon}{2}\right)^2+\frac{\tilde{Q}}{2}}. \quad (3.9)$$

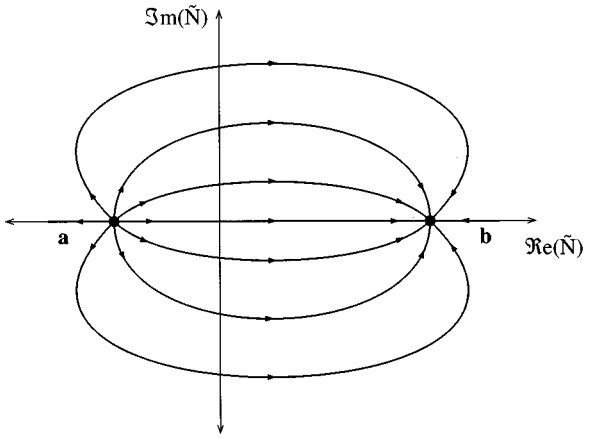

FIG. 2. Schematic representation of the phase space of the deterministic part of the laser equation. Of particular importance, there is a single trajectory from a that escapes to $-\infty$, before returning from $+\infty$ to b.

We use the Stratonovich form of the equations since this is the most natural form in which to implement them in a numerical algorithm.

The deterministic part of Eq. (3.8) contains the essence of the problem. An equation of the form

$$\frac{d\tilde{N}}{dt}=-\xi(\tilde{N}-a)(\tilde{N}-b) \tag{3.10}$$

has two critical points, one at a and the other at b. Linearizing about these points will show them to be a simple repellor (we shall label this as a) and a simple attractor (labeled b). Each point has two eigenvalues of equal magnitude but opposite sign [$\mp\xi(a-b)$, respectively] with orthogonal eigenvectors each parallel to a coordinate axis.

The effect of the nonlinearity is to wrap the trajectories around from the repellor to the attractor; see Fig. 2. There is a single trajectory from a (the repellor), which escapes to $-\infty$, before returning from $+\infty$ to b. Since a crucial assumption in the derivation of the positive P representation was that the current at infinity was zero, this trajectory plays the critical role in the validity of the solutions.

The solution of Eq. (3.10) with initial condition $\tilde{N}(t=0)=n$ is [52]

$$\tilde{N}(t,n)=a+\frac{(b-a)(n-a)}{n(1-e^{\lambda t})+be^{\lambda t}-a}, \tag{3.11}$$

where $\lambda=\xi(b-a)$. The solution clearly has a singularity as a function of n at

$$n=\frac{a-be^{-\lambda t}}{1-e^{-\lambda t}}. \tag{3.12}$$

This singularity starts off at negative infinity and moves along the negative real axis reaching the critical point a at $t=\infty$. The singularity will not affect the solution given an initial distribution that does not contain any point x on the real axis at $x\leqslant a$.

The Gaussian initial condition can be thought of as an appropriately weighted sum of concentric rings of radius r. The average photon number, averaged over a ring $\langle\tilde{N}(t)\rangle_r$ is given by [52]

$$\langle\tilde{N}(t)\rangle_r=\frac{1}{2\pi i}\oint_{C_r}\frac{dn}{n}\tilde{N}(t,n), \tag{3.13}$$

where the contour of the integral C_r is over the circle $|n|=r$. As long as $\tilde{N}(t,n)$ is analytic in n inside C_r we can use contour integration to get

$$\langle\tilde{N}(t)\rangle_r=\tilde{N}(t,0). \tag{3.14}$$

Thus the mean value will be the solution for the deterministic equation with the vacuum initial condition. However, $\tilde{N}(t,n)$ *does* have a singularity [Eq. (3.12)], and this will hit a circle of radius r at the point $n=-r$, at the time

$$t_e=\frac{1}{\lambda}\ln\left|\frac{r+a}{r+b}\right| \tag{3.15}$$

[at the same time we find the solution for the initial condition $\tilde{N}(t,-r)$ escapes to infinity]. Taking into account that the singularity is now within the contour, we can evaluate the contour integral to get the discontinuous solution

$$\langle\tilde{N}(t)\rangle_r=\tilde{N}(t,n=0)+\begin{cases}0, & t<t_e\\ G(t), & t>t_e,\end{cases} \tag{3.16}$$

where

$$G(t)=\frac{e^{\lambda t}(a-b)^2}{(1-e^{\lambda t})(ae^{\lambda t}-b)}. \tag{3.17}$$

In summary, the initial distribution evolves so that at the time t_e it passes through a point at infinity. At this time it is no longer valid to drop the boundary terms. Prior to this time the boundary terms are necessarily negligible since the distribution is bounded. Hence the solution of the positive P representation is correct up to the time t_e and is incorrect thereafter. Only one trajectory (set of measure zero) actually escapes to infinity and in practice this trajectory never appears in simulation. Omitting spiking trajectories from the simulation results clearly will not help since it is the dynamics that are at fault. We expect problems to appear at the earliest time a deterministic trajectory *can* escape. Nearby trajectories to the trajectory that actually escapes will give an indication of the time the distribution results break down.

B. Full stochastic case

Consider now a small stochastic influence—this will distort the circle so that we would expect to see a broadening of the jump in the mean, since in each of the instances averaged over, the jumps occur at slightly different times. The more noise present the more broadened the discontinuity. This will have the effect of ''washing out'' the precise time at which the solution jumps. We have solved Eqs. (3.8) with trajectories starting from a randomly chosen point along a circle centered at the origin. Although large excursions into ''unphysical'' regions of phase space (spikes) were present in the

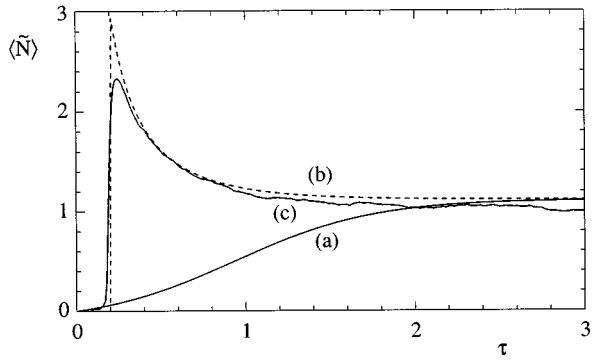

FIG. 3. Comparison of analytic treatment for the deterministic equation with the simulation of the stochastic equation (3.8) for the laser. Curve (a), mean photon number with an initial delta distribution centered at the origin; curve (b) (dashed line), analytic curve from Eq. (3.16), and curve (c), mean photon number for 500 trajectories from an initial 1000 points distributed on a circle; $\Delta t = 5\times10^{-3}$. Curves ($b$) and ($c$) are both for an initial circle of radius 2. Parameters: $\epsilon = 1$ and $\tilde{Q} = 0.25$.

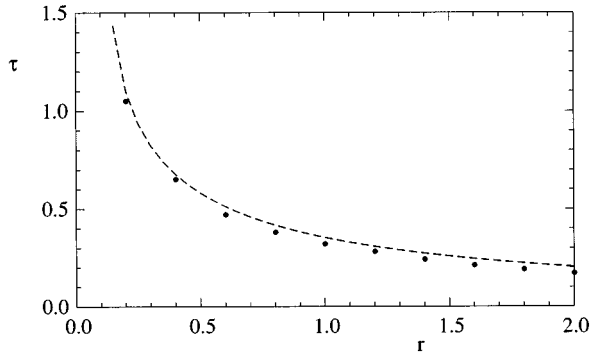

FIG. 4. Laser equation with initial ring distributions of different radii $r = |N|$. Plotted is the earliest out of 40 trajectories to satisfy $\mathrm{Re}(\tilde{N}) \leqslant -20$ (dots) against r. These trajectories correlate well with the time t_e in Eq. (3.16) (dashed line). Simulation parameters: $\Delta t = 10^{-3}$, $\epsilon = 1$, and $\tilde{Q} = 0.25$.

simulations none actually escaped to infinity; rather, they looped around and back towards the attractor. In Fig. 3 we compare this full stochastic case with the results of the analytic treatment of the previous section, and find that the discontinuity in the average photon number is still present and occurs approximately at the time t_e. The results for trajectories starting from an initial Gaussian will be reproduced by summing over the results for various rings, each with an appropriate weighting.

There is then no doubt that the reason for the failure of the broad Gaussian initial distribution is that there is a significant component of points on rings larger than the critical radius, so that boundary terms are no longer negligible after the time t_e.

C. Numerical signatures

In this section we demonstrate the presence of numerical signatures that signal the breakdown of the simulation. We have found that the presence of spikes, an increase in the variance, and the radial distribution taking on a power-law form ($P \sim |\tilde{N}|^{-n}$) herald a breakdown of the positive P representation.

1. Presence of spikes

Starting from an initial ring distribution the stochastic trajectories will occasionally make large excursions into regions of phase space near the unstable manifold, that is spikes will occur. The definition of a spike is necessarily qualitative in that the degree to which a trajectory makes a ''large excursion'' is an arbitrary amount. Here and in the rest of the paper we will generally require that a spike be a trajectory that makes an excursion several times larger than the initial and the steady-state values, and in a direction towards the trajectory that escapes to infinity in the deterministic equations.

We have found that the *earliest* of these spikes correlates well with the analytically calculated time t_e based purely on the deterministic equation. In Fig. 4 a ''large excursion'' was defined by $\mathrm{Re}(\tilde{N}) \leqslant -20$; as can be seen this closely tracks the theoretical curve. These numerically obtained times then provide a reliable estimate of t_e.

2. Increase in the statistical error

Given the presence of these large excursions into phase space it is natural to expect an increase in the variance of the distribution. Monitoring the statistical error can be achieved with little outlay in computation. An increase in the statistical error of the distribution can help indicate the presence of spiking trajectories. Of course, if a distribution develops a power-law tail (next section) then an increase in the statistical error will be a natural consequence.

Starting from an initial distribution on a ring we monitored the mean photon number and the variance (Fig. 5) and found that the variance indeed does increase dramatically at the time of the discontinuity in the deterministic equation (t_e).

3. Development of a power-law tail

In order to give a more precise description of what is happening, it is useful to investigate the probability distribu-

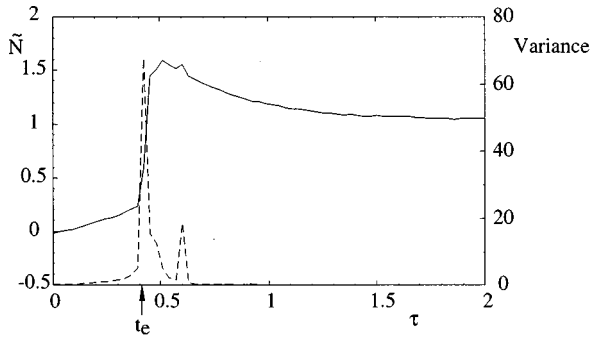

FIG. 5. The variance of the photon number for the laser (dashed line) increases dramatically at the time t_e when the mean photon number also undergoes a large change (solid line). There were 3000 trajectories from an initial ring distribution of radius $r = 0.8$. Simulation parameters $\Delta t = 10^{-3}$, $\epsilon = 1$, and $\tilde{Q} = 0.25$.

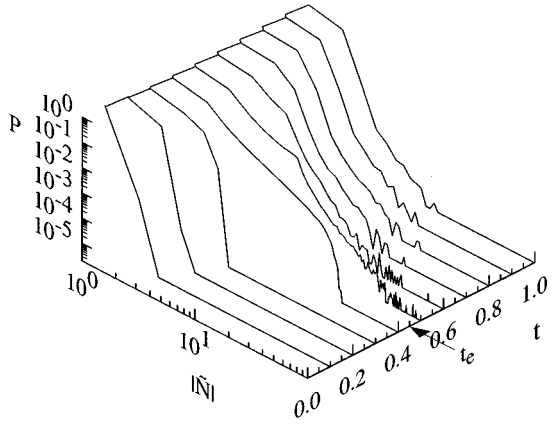

FIG. 6. Locations of trajectories for the laser binned according to their radii ($r=|\tilde{N}|$) at specific instances in time. Dividing by the total number of trajectories (5×10^5) yields an estimate for the probability. This figure shows the behavior of the tails of the probability distribution. A power-law distribution will be a straight line (indicated by the data at the time t_e with a value of about r^{-3}). The time arrowed is the time t_e described in the text. Simulation parameters: $\Delta t=10^{-3}$, $\epsilon=1$, and $\tilde{Q}=0.25$. Trajectories started from an initial ring distribution of radius $r=0.8$. Note that the graph has a ''false bottom'' at the level of a single trajectory.

tions of points being simulated. In particular, the behavior of the tails of the distribution with time can be explored by binning the trajectories into a set of concentric bins with $|\tilde{N}|$. Over a sufficient number of trajectories this will give an estimate of the probability of a trajectory reaching a certain radius. If the distribution falls off exponentially (or faster) with the radius in phase space then there will certainly be no problems with boundary terms. However, if the distribution falls off as a power law then boundary terms may present a problem unless the power is sufficiently high.

Figure 6 suggests that the tail end of the distribution for the laser begins to fall off as a power law at the same time t_e that the onset of spiking was observed. The value of the power is about $|\tilde{N}|^{-3}$, which is the value expected from an analysis of the equations (see Sec. IV A for more details).

The appearance of a power-law tail at the time t_e can be expected to invalidate the partial integration required to derive the Fokker-Planck equation from a master equation. From this we can conclude that the solution given *after* the time t_e is not a valid solution to the master equation with the given initial condition. The power-law tail quickly disappears after this time. We surmise that the solution after t_e is correct for a distribution *starting* from the distribution achieved after the time t_e, but not for the initial distribution at the time $t=0$.

Hence the positive P representation remains valid up until the time when the boundary terms become significant, and there is ample evidence in the numerical work to identify this time independently of analytical treatment.

We conclude then that Schack and Schenzle used an unreasonably broad initial distribution, by confusing the use of scaled with unscaled variables. In doing so, the dynamics of the equation was affected by the presence of a trajectory that could escape to infinity in the deterministic phase space. This singularity is intimately related to the presence of boundary terms, so that the derivation of their Fokker-Planck equation was not valid in this limit. With the correct initial distribution, and a reasonable choice of scaling parameter, the problem is nonexistent. This should not be taken as an argument that boundary term corrections do not exist. In fact, the extremely unphysical conditions used by these authors have a useful role in illustrating potential limitations of positive P simulations. However, any small corrections from this source will be completely negligible compared to those due to the standard truncations already introduced, for typical laser parameters.

IV. THE DRIVEN ONE- AND TWO-PHOTON ABSORBER

The model we consider in this section is a cavity that is driven by coherent radiation and damped by one- and two-photon losses to a zero-temperature bath. It is also possible to arrive at the same equations by considering second-harmonic generation with the harmonic mode adiabatically eliminated, as was considered in Ref. [45]. We will demonstrate that the breakdown of the positive P representation in this model has the same mechanism as uncovered in the previous section. Not surprisingly, all the numerical indicators previously discussed will also be present at low damping, with the addition of a definite power-law signature, indicating a radial dependence of the distribution that goes to zero only as a power law of the radius. This can be attributed to the presence of an isolated singular trajectory in the deterministic dynamical equations.

Following standard techniques, this system can be described by the master equation

$$\frac{\partial\rho}{\partial t}=[Ea^\dagger-E^*a,\rho]+\kappa_1(2a\rho a^\dagger-a^\dagger a\rho-\rho a^\dagger a)$$
$$+\frac{\kappa_2}{2}(2a^2\rho a^{\dagger2}-a^{\dagger2}a^2\rho-\rho a^{\dagger2}a^2), \tag{4.1}$$

where κ_1 is the rate of one photon loss and κ_2 is the rate of two photon loss. We now introduce a scaled version of this equation with time scaled by κ_2 and hence $\tau=\kappa_2 t$, $\gamma=2\kappa_1/\kappa_2$, and $\epsilon=E/\kappa_2$ ($\kappa_2\neq0$). This helps to clarify the dynamics, and introduces a dimensionless parameter γ, which describes the degree of nonlinearity involved. The damping is entirely nonlinear when $\gamma=0$ and the proportion of linear damping increases as γ increases. Hence we have chosen to emphasize the nonlinearity in the equations

$$\frac{\partial\rho}{\partial\tau}=[\epsilon a^\dagger-\epsilon^*a,\rho]+\frac{\gamma}{2}(2a\rho a^\dagger-a^\dagger a\rho-\rho a^\dagger a)$$
$$+\frac{1}{2}(2a^2\rho a^{\dagger2}-a^{\dagger2}a^2\rho-\rho a^{\dagger2}a^2). \tag{4.2}$$

Applying the positive P procedure and discarding the boundary terms, results in the Fokker-Planck equation

$$\frac{\partial P(\alpha,\alpha^+)}{\partial \tau}=\left\{-\frac{\partial}{\partial\alpha}\left(\epsilon-\frac{\gamma}{2}\alpha-\alpha^2\alpha^+\right)-\frac{\partial}{\partial\alpha^+}\left(\epsilon^*-\frac{\gamma}{2}\alpha^+-\alpha^{+2}\alpha\right)-\frac{1}{2}\left[\frac{\partial^2}{\partial\alpha^2}\alpha^2+\frac{\partial^2}{\partial\alpha^{+2}}\alpha^{+2}\right]\right\}P(\alpha,\alpha^+), \quad (4.3)$$

which in turn is equivalent to the Ito stochastic differential equations

$$d\alpha=(\epsilon-\tfrac{1}{2}\gamma\alpha-\alpha^2\alpha^+)d\tau+ i\alpha dW_1, \quad (4.4a)$$

$$d\alpha^+=(\epsilon^*-\tfrac{1}{2}\gamma\alpha^+-\alpha^{+2}\alpha)d\tau+ i\alpha^+ dW_2, \quad (4.4b)$$

where dW_1 and dW_2 are independent Wiener increments.

It is easier to study these equations in the various limits corresponding to the models that have previously appeared in the literature, namely, the damped nonlinear absorber and the driven nonlinear absorber [43–46,52]. We will first focus on the damped nonlinear absorber, without a driving term.

A. The damped nonlinear absorber

This model demonstrates that the positive P representation can yield incorrect results that are not due to the numerical algorithms, but intrinsic in the method itself [43]. With $\epsilon=0$ in Eq. (4.4) we arrive at the damped nonlinear absorber treated in [43–45,52]. This model is best treated numerically using the equations for the photon number, $N=\alpha^+\alpha$. We choose to use the Stratonovich calculus here for the best numerical accuracy, and obtain the resulting Stratonovich stochastic equation, where time has been scaled to remove a factor of 2, with $\tau=\tau'/2$ and $\langle dW'^2\rangle=d\tau'$:

$$dN=-N\left(N-\frac{1-\gamma}{2}\right)d\tau'+iNdW'. \quad (4.5)$$

Equation (4.5) is known to produce the wrong steady state for $\gamma\leqslant 1$, and the correct steady state but with some transient differences for $1<\gamma\lesssim 2$ [43,44,52]. In fact, the positive P representation will initially give accurate results but will at some time during the simulation depart from the correct answer as in Fig. 7. We have labeled the approximate time of this departure as t_e (note that in this section t_e is a numerically estimated time, defined as the time the positive P solution becomes distinct from the master equation solution).

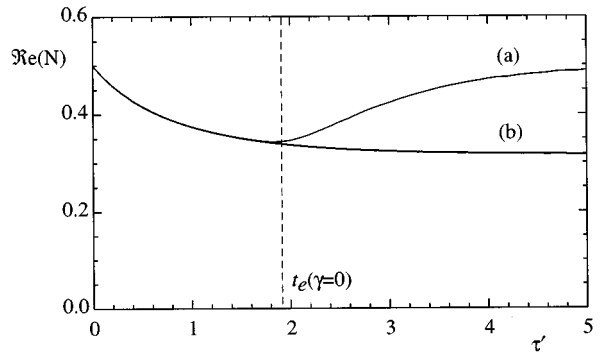

FIG. 7. Comparing the master equation solution against the positive P solution for the damped nonlinear absorber with $\gamma=0$. Curve (a) the mean value of Re(N) using the positive P representation; curve (b) the master equation solution calculated in a truncated number state basis.

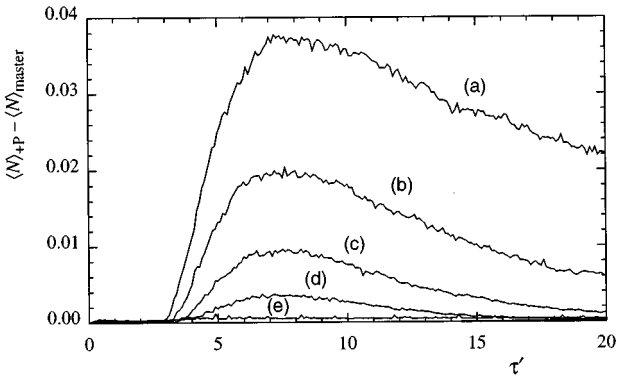

FIG. 8. Some transient differences between positive P solution and the master equation for the damped nonlinear absorber. (a) $\gamma=1.1$, (b) $\gamma=1.2$, (c) $\gamma=1.3$, (d) $\gamma=1.5$, and (e) $\gamma=1.7$. Clearly, as the amount of linear damping is increased both treatments yield the same result. Positive P simulation parameters: $\Delta t=0.005$, 5×10^5 trajectories with initial condition 0.5.

The steady state of the positive P solution for N with $\gamma\leqslant 1$ is $\langle N\rangle_{ss}=(1-\gamma)/2$. It falls linearly, as γ goes from 0 to 1, from $\langle N\rangle_{ss}=0.5$ to $\langle N\rangle_{ss}=0$. For $\gamma>1$ the steady state is always zero. The solution of the master equation on the other hand always decays to zero with $\gamma>0$—all the photons eventually leak out. With $\gamma=0$ the initial coherent state can be considered a superposition of even and odd photon number states; the even number states decay to zero, the odd decay to one. The steady state of the master equation for $\gamma=0$ is the weighted average between zero and one, of the original even and odd number states, respectively. In summary, the difference between the positive P and master equation solutions in the steady state will disappear linearly as γ is increased with apparent equality being achieved for $\gamma\geqslant 1$. There is also a transient difference, but this is small and also disappears for values of γ not much larger than one, see Fig. (8)—this is consistent with the work of Smith and Gardiner [43], who found that a positive P representation

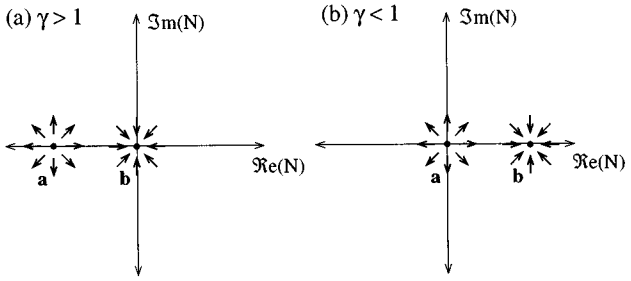

FIG. 9. Behavior of the critical points of the deterministic part of the stochastic differential equation for the damped nonlinear absorber. The position and stability of the fixed points are determined by the parameter γ: (a) $\gamma>1$ and (b) $\gamma<1$.

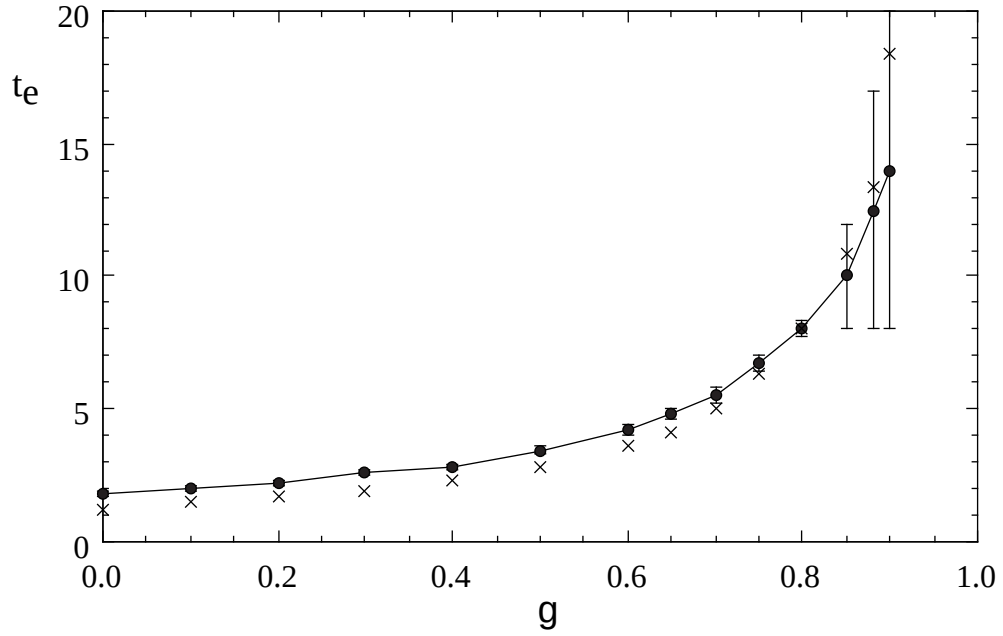

FIG. 10. Damped nonlinear absorber showing a comparison between the time at which the positive P solution starts to deviate significantly from the master equation solution (joined dots) and the earliest spike time out of a set of 10 000 spikes (crosses). A spike was defined as the trajectory that reached $\mathrm{Re}(N)\leqslant -2$. For each γ the initial distribution was a delta distribution centered at $(1-\gamma)/2$. The error bars are due to the difficulty in estimating the time at which the two methods began to differ in the data as γ approached 1.

gave correct results for stationary and time-dependent solutions for $\gamma\geqslant 2$.

This behavior, of achieving the wrong steady state dependent on γ, can be understood by examining the deterministic equation alone. The form of the deterministic equation is the same as Eq. (3.10) treated in the previous section, so we expect that the unbounded trajectory from the repellor will play an important role. Though here we are simply dropping the noise terms in order to allow some analytical insights, Appendix A presents a modification of Eq. (4.5), which is entirely treatable analytically.

Clearly, the position and stability of the two critical points in phase space for the model depend on the value of γ. The position of the critical points in turn affects the likelihood of the distribution reaching the unbounded trajectory from the repellor a. There are two principal situations to consider (refer also to Fig. 9).

(1) $\gamma>1$. In the phase space, a (the repellor) lies on the negative real axis at $(1-\gamma)/2$ and b (the attractor) is at the origin. Again, there is a single deterministic trajectory (of measure zero) that can escape to $-\infty$ from a along the negative real axis. For a trajectory to have a reasonable probability of escape to infinity, either the initial distribution has to be broad enough to encompass the negative real axis beyond a, or the noise must broaden the distribution to that extent. The deterministic flow of the equations, on the other hand, opposes this motion and condenses the distribution onto the attractor b. The noise at b vanishes since it is located at the origin, so that once the distribution is in the neighborhood of b the diffusion is suppressed. Increasing the value of γ puts the repellor further and further away. Hence provided the initial distribution is narrow enough that it does not encompass the unbounded trajectory from a there will be very little probability of the distribution exploring that region in phase space. Hence the positive P representation gives increasingly better results for higher γ (corresponding to more linear absorption). The boundary term is exponentially suppressed in the large γ limit, due to the existence of an increasingly large potential barrier at a. Since the noise term is pure imaginary and can by itself only change the phase of N, not its magnitude, then for any $\gamma>1$ there exists a region including the origin such that initial ensembles chosen in that region can never leave it, and hence the results are exact. For example, the region $|N|<1$ is appropriate for $\gamma\geqslant 3$.

(2) $\gamma<1$. The repellor a is now at the origin and the attractor b lies on the positive real axis at $(1-\gamma)/2$. The noise at b no longer vanishes, so as the distribution condenses in the neighborhood of b it still experiences some diffusion. There is then a significant chance of escaping to negative infinity by the process of activated escape over a (low) barrier. Hence it is not surprising that the positive P simulation gives an incorrect result, as the tail of the distribution extending to $N=-\infty$ is not suppressed in this case.

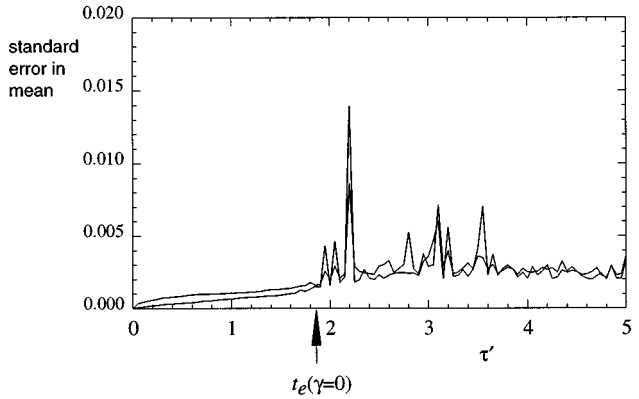

FIG. 11. Standard error in the mean photon number plotted against time for the damped nonlinear absorber. Parameters $\gamma=0$ with an initial delta distribution at $N=0.5$. The arrowed time is when the positive P solution starts to deviate significantly from the master equation solution. The variances in the real and in the imaginary parts are shown.

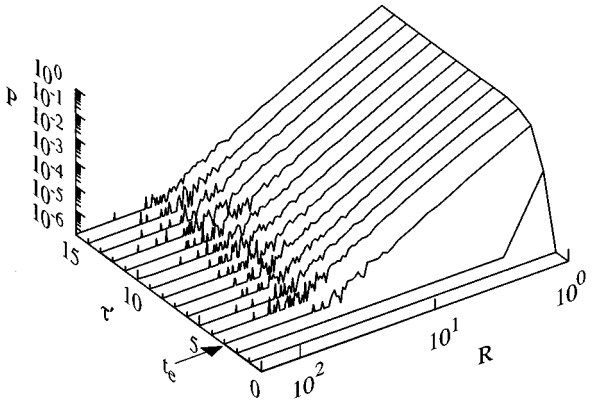

FIG. 12. Locations of trajectories for the damped nonlinear absorber binned according to their radii ($r=|N|$) at specific instances in time. The data indicate a power-law tail developing after a certain time of the form r^{-3}. The time arrowed is when the positive P and master equation solutions for N start to deviate significantly from each other. $\gamma=0.4$ and 1×10^6 trajectories were used from an initial condition of 0.3.

We now analyze this problem according to the numerical signatures used earlier.

1. Presence of spikes

The time at which the positive P solution deviates significantly from the master equation solution is again strongly correlated with the observation of the onset of spiking. In Fig. 10 we compare the positive P solution with the master equation solution. The initial distribution was a delta distribution centered on the attractor b. For each value of γ we collected 10 000 spikes [defined as a trajectory with $\mathrm{Re}(N)\leqslant-2$]. The first of these spikes to occur in time is plotted together with the estimated time t_e. We estimate t_e graphically from a plot of the positive P solutions superimposed on the master equation solution. As can be seen the earliest spike provides accurate warning of the existence of boundary terms, making the positive P method invalid in this case.

2. Increase in the statistical error

Monitoring the statistical error in a simulation produced Fig. 11. The time t_e has been indicated on the plot. The trajectories that took large excursions in the simulation clearly left their mark in the statistical error of the ensemble.

3. Development of a power-law tail

Since the previous two signatures are present it is prudent to directly explore the nature of the tails of the distribution. Simply by binning trajectories into concentric rings, we can explore for a power-law tail. From Ref. [43] we expect that since in the inverse variables, $v=1/N$, the distribution in phase space at the origin is a smoothly varying function, then space at the origin is a smoothly varying function, then, with $r=|N|$,

$$P(r)=\frac{1}{r}P(v)\left|dv/dN\right|\simeq 1/r^3. \tag{4.6}$$

Figure 12 indeed demonstrates such a power-law tail developing at the time t_e.

A distribution with a power-law tail will invalidate the neglect of the boundary terms, and hence the Fokker-Planck equation cannot be guaranteed to give the same result as the master equation.

Again, in conclusion, the positive P representation yields correct solutions provided that the dynamics do not explore the region near the unstable deterministic trajectory. This situation will occur for values of γ much greater than 1. We note that in experimental two-photon absorbers, values of γ of order 10^6-10^{10} might be regarded as being typical in current practice, although there appears to be no fundamental reason for this.

B. Driven nonlinear absorber ($\gamma=0$)

Another limit in which Eqs. (4.4) have been presented as a failure of the positive P representation is when the damping in entirely nonlinear and a coherent driving term is also included [46]; this can be seen in Fig. 13. That this model should fail is of no surprise since with no driving it is merely the same model discussed in the previous section with the most extreme parameter choice—$\gamma=0$. The effect of the driving will then enhance the tendency of trajectories to explore the region of phase space near the unbounded deterministic trajectory, leading to a worse situation.

Taking $\gamma=0$ and $\epsilon\neq0$ in Eqs. (4.4) leads to (in the Stratonovich form)

$$d\alpha=(\epsilon+\tfrac{1}{2}\alpha-\alpha^2\alpha^+)d\tau+i\alpha dW_1, \tag{4.7a}$$

$$d\alpha^+=(\epsilon^*+\tfrac{1}{2}\alpha^+-\alpha^{+2}\alpha)d\tau+i\alpha^+dW_2. \tag{4.7b}$$

dW_1 and dW_2 are independent Wiener processes.

1. Presence of spikes

Again, the conjecture that the earliest spike observed is a good measure of when the positive P solution begins to fail is borne out by simulation—see Fig. 14.

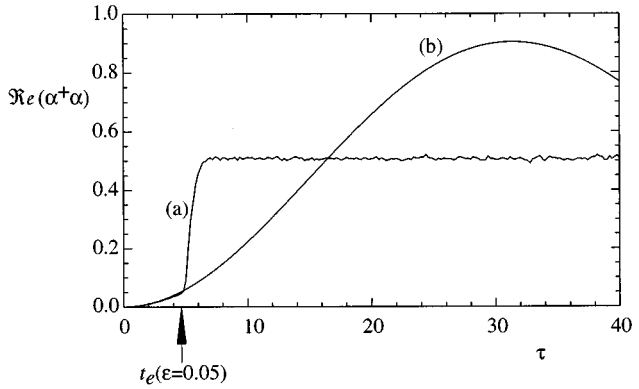

FIG. 13. Comparison between the master equation solution and the positive P representation solution for the driven nonlinear absorber. (a) The positive P simulation with 10 000 trajectories with the origin as initial condition and (b) direct simulation of the master equation in a truncated number state basis. Parameter: $\epsilon = 0.05$.

2. Increase in the statistical error

In Fig. 15 the standard error in the mean values shows a significant jump following the time the positive P solution begins to depart from the master equation (time t_e).

3. Development of a power-law tail

Examining the shape of the tails of the distribution in the variable $R = \sqrt{|\alpha|^2 + |\alpha^+|^2}$ again reveals that a power law develops at the time t_e; see Fig. 16.

4. Increasing the linear damping

By allowing some linear damping $\gamma > 0$ we can regain a more physical model. Here we start to explore the full set of equations (4.4). It is easy to show that the difference between the positive P representation solution and the master equation solution rapidly vanishes as γ increases as depicted in Fig. 17.

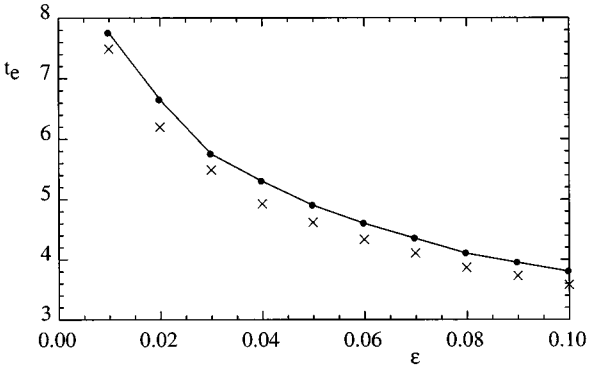

FIG. 14. Comparison of the time at which the positive P simulation (of the photon number) significantly departs from the master equation solution with the time of the earliest detected spike in the driven nonlinear absorber. The joined dots are when the two methods deviate by more than 0.01 unit (in photon number); the crosses are the earliest times a trajectory reaches $\mathrm{Re}(N) \leqslant -2$ out of an ensemble of 10 000.

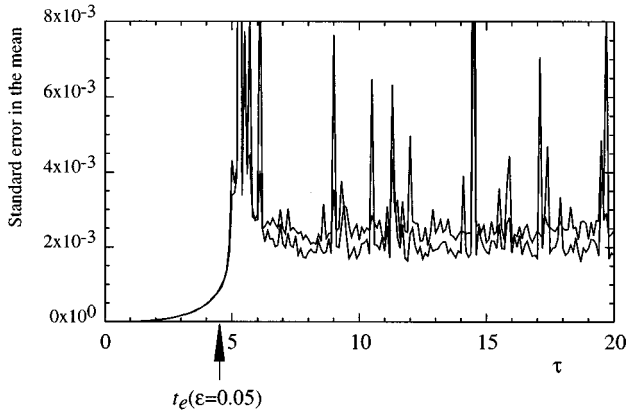

FIG. 15. A sudden increase in the standard error of the mean photon number occurs at the same time at which the positive P solution departs from the master equation solution (arrowed). Parameter: $\epsilon = 0.05$. The variance in the real and in the imaginary parts is shown.

In this case, as in the previous section, the positive P representation gives accurate results initially but breaks down after a well-defined time, which can be determined numerically. As previously, the boundary term problem appears restricted to cases of very small linear damping and low photon numbers.

V. THE ANHARMONIC OSCILLATOR

The damped anharmonic oscillator has received some attention in the past, either as a model of molecular vibrations, or as a theory of a driven nonlinear Fabry-Pérot interferometer [53]. In this section, we only deal with the exactly soluble case of a damped anharmonic oscillator without external driving. Although this is a trivial example, it is the simplest possible physical problem with nonlinearity and damping present. We find that the positive P representation gives reliable results for this model. Numerically though,

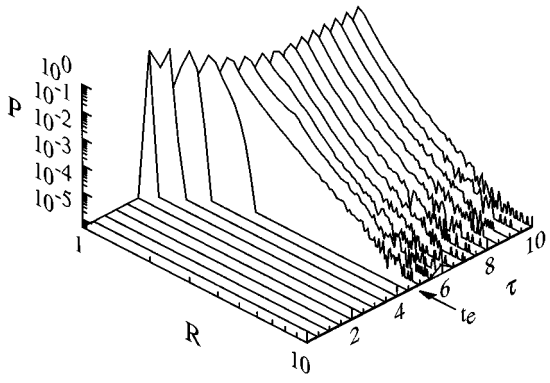

FIG. 16. In the driven nonlinear absorber the radial position of a trajectory was accumulated at various times over 200 000 runs. The logarithm or R is plotted against the logarithm of P, the probability of arriving at a certain radius. A straight line indicates a power law. After the time t_e the tails have a power-law structure, in the range R^{-5}–R^{-6}. Note that, since $R \simeq r^2$, this is similar to the earlier cases. The initial condition was the origin and $\epsilon = 0.05$.

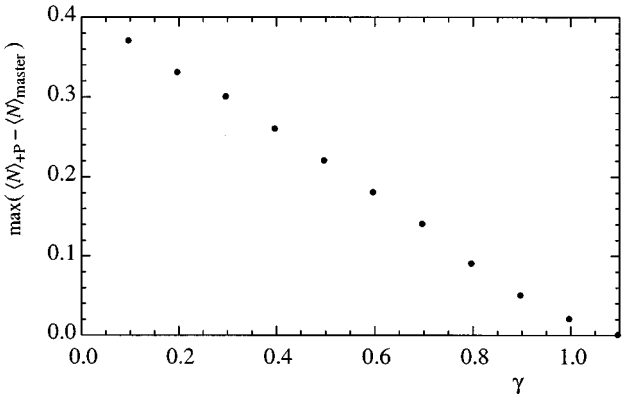

FIG. 17. Maximum difference between positive P simulation and the master equation solution of the photon number (to the nearest 0.01) plotted against γ. This plot shows that as the linear damping is increased in the driven nonlinear absorber the positive P solution and master equation solution converge. For $\gamma>1.1$ there was no detectable difference.

there are practical difficulties to be surmounted and care must be taken in interpreting the numerical signatures.

In the interaction picture and under the Markov-Born approximations we start from the following master equation for the reduced density operator:

$$\frac{\partial\rho}{\partial t}=\kappa_1(2a\rho a^\dagger-a^\dagger a\rho-\rho a^\dagger a)-\frac{i}{2}\kappa_2[a^{\dagger 2}a^2,\rho]. \tag{5.1}$$

Again, scale time by κ_2 and so introduce $\tau=\kappa_2 t$, $\gamma=2\kappa_1/\kappa_2$ $(\kappa_2\neq 0)$ to get

$$\frac{\partial\rho}{\partial\tau}=\frac{\gamma}{2}(2a\rho a^\dagger-a^\dagger a\rho-\rho a^\dagger a)-\frac{i}{2}[a^{\dagger 2}a^2,\rho]. \tag{5.2}$$

This equation is easily solved for photon number with the result

$$\frac{d\langle a^\dagger a\rangle}{d\tau}=\mathrm{Tr}\{a^\dagger a\rho\}=-\gamma\langle a^\dagger a\rangle. \tag{5.3}$$

The usual assumption of vanishing boundary terms in the positive P representation time evolution yields the Fokker-Planck equation

$$\frac{\partial P}{\partial\tau}=\left\{-\frac{\partial}{\partial\alpha}\left(-\frac{\gamma}{2}\alpha-i\alpha^+\alpha^2\right)-\frac{\partial}{\partial\alpha^+}\left(-\frac{\gamma}{2}\alpha^++i\alpha\alpha^{+2}\right)+\frac{1}{2}\left[\frac{\partial^2}{\partial\alpha^2}(-i\alpha^2)+\frac{\partial^2}{\partial\alpha^{+2}}(i\alpha^{+2})\right]\right\}P. \tag{5.4}$$

This Fokker-Planck equation is then equivalent to the Ito stochastic differential equations

$$d\alpha=\left(-\frac{\gamma}{2}\alpha-i\alpha^2\alpha^+\right)d\tau+\sqrt{-i}\alpha dW_1, \tag{5.5a}$$

$$d\alpha^+=\left(-\frac{\gamma}{2}\alpha^++i\alpha^{+2}\alpha\right)d\tau+\sqrt{i}\alpha^+dW_2, \tag{5.5b}$$

where dW_i are real Gaussian stochastic processes satisfying $\langle dW_i dW_j\rangle=d\tau\delta_{i,j}$.

From Eqs. (5.5) we can write a single stochastic differential equation in the variable $N=\alpha^+\alpha$,

$$dN=-\gamma N d\tau+N(\sqrt{-i}dW_1+\sqrt{i}dW_2). \tag{5.6}$$

As all stochastic variables in an Ito stochastic differential equation are uncorrelated with the noise terms at the same time, the stochastic mean value of N must follow the equation

$$d\langle N\rangle=-\gamma\langle N\rangle d\tau. \tag{5.7}$$

Hence, the exact master equation solution is clearly recovered for the photon number.

An interesting observation is that while Eq. (5.6) has noise terms and hence diffusion in the phase space, the equivalent equation (5.7) does not. This can lead to problems, since at some stage the diffusive spreading of the distribution may be great enough to cause the statistical errors to become significant in a simulation.

In order to treat this, consider the new stochastic variable $M=|N|^2$. This has no corresponding physical observable (it is not an analytic function of N), but $\sqrt{\langle M\rangle}$ gives a measure of the mean distribution radius in N space. Following the usual Ito rules for products of stochastic variables, $\langle M\rangle$ satisfies the equation

$$d\langle M\rangle=2(1-\gamma)\langle M\rangle d\tau. \tag{5.8}$$

We see here an indication of difficulties that can occur in stochastic simulations, even when there is a complete theoretical equivalence of the Fokker-Planck and master equations. If $\gamma<1$, then the mean distribution radius grows in time. This has no effect on ensemble averages for infinite ensembles, but clearly can give rise to increased sampling errors at long times, for the finite samples used in numerical simulations. In fact, it is easy to show that all moments of the distribution in N remain finite if initially finite. Thus, the distribution is at least exponentially bounded, and hence has no boundary terms. This is compatible with the fact that the stochastic equations give exactly identical results to the master equation, as expected.

However, each radial moment has a critical damping, below which it exhibits steady growth in time. This is an indication of increased sampling error at low damping and long times, even though the mean values remain correct, as shown in Fig. 18.

A. Numerical signatures

Even though there are no boundary terms in these equations, we include here an analysis of the numerical signatures that can indicate boundary terms, as a cautionary tale. As we see, it is possible for the simplest numerical signatures to apparently indicate boundary terms, even when they do not exist. A careful quantitative treatment shows that, as expected, boundary terms are not present. Despite this, the growth of sampling error with time (for small or zero linear damping) can mimic the effect of boundary terms.

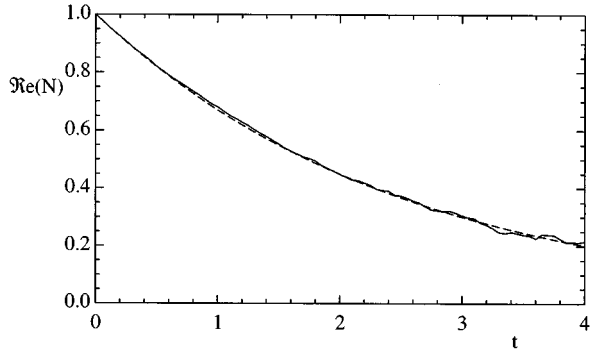

FIG. 18. Anharmonic oscillator: the result of a simulation of Eqs. (5.6) with 50 000 trajectories with a coherent state having one photon initially in the cavity (solid line). The numerical parameters are $\Delta t=0.01$ and $\gamma=0.4$. Analytic solution given by Eq. (5.7) (dashed line).

1. Presence of spikes

For this model a ''spike'' was arbitrarily defined as a trajectory that explored the phase space outside the radius $|N|>50$. Trajectories of this sort were observed early in the simulation—with no apparent lower bound on the first ''spike'' time, for large samples. We emphasize that these do not originate from the presence of a deterministic unstable trajectory. Instead, they are simply due to the dynamics of the multiplicative stochastic process involved here. However, in this case the large radius trajectories belong to a distribution that is sufficiently well bounded to give rise to exact results, without boundary terms.

2. Increase in the statistical error

As can be seen in Fig. 19, the quantity $\langle|N|^2\rangle$ increases in keeping with the predictions from the analytic equations. There is no threshold time for this to take place, since it is due to a diffusive process.

3. Development of a power-law tail

Because of the diffusive spreading, for *any* given distance scale there is a characteristic time after which the tails of the radial distribution can take on the character of a power law. On larger distance scales, exponentially bounded tails are

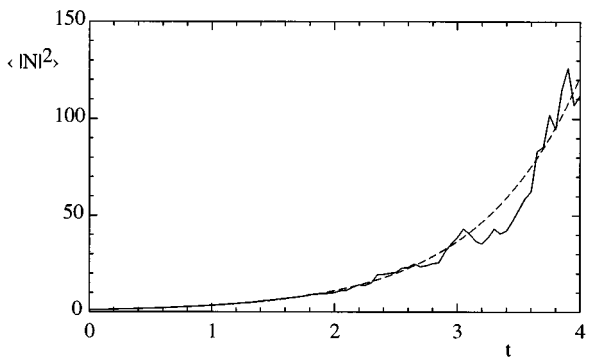

FIG. 19. Mean value of $|N|^2$ (solid line) for 50 000 trajectories together with the solution to Eq. (5.8) (dashed line). The numerical parameters are $\Delta t=0.01$ and $\gamma=0.4$.

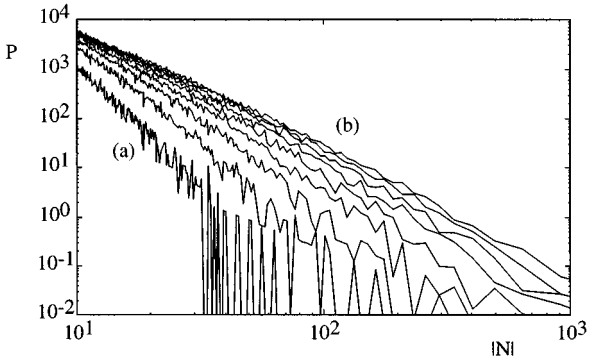

FIG. 20. Examining the radial distribution of 1 800 000 trajectories at various times for the anharmonic oscillator. This reveals a dropoff with radius $r=|N|$ faster than a power law (a power law would be indicated by a straight line). The times are (a) $t=0.8$ through to (b) $t=4$. The numerical parameters are $\Delta t=0.01$ and $\gamma=0.4$.

recovered. However, it becomes increasingly difficult to numerically explore the nature of the tails at larger and larger $r=|N|$—because trajectories reaching large r become rarer. Nevertheless, there is no *sudden* appearance of a power-law tail. A careful examination reveals that the distribution always falls off faster than a power law at large radius, as in Fig. 20.

4. Increasing the linear damping

Finally as the amount of linear damping is increased, the numerically difficult quantum features in the simulation gradually disappear. That is, ''spiking'' is no longer observed, the statistical error stays small, and the distribution tails are reduced.

In conclusion, the positive P representation is useful in this nonlinear example, although the efficiency (in terms of computing time to obtain the required sampling error) is greatest at levels of reasonable linear damping. This can be checked by the absence of the numerical signatures discussed, even though there is no question of boundary terms in this case. It is useful to compare this situation with the more traditional representations. None of these has stochastic equations. The P and Q representations have non-positive-definite Fokker-Planck equations, while the Wigner equation is of third order, which automatically prevents any stochastic interpretation of the propagator. By comparison, an exact stochastic simulation is numerically possible, without boundary-term corrections, using the positive P representation. While this example is a somewhat trivial one, the same principles apply to problems that are less tractable—including the original calculations of nonclassical features in nonlinear interferometers and quantum solitons, in which the same effects are present.

VI. THEORETICAL FRAMEWORK OF THE PROBLEM

The aim of the positive P representation is to generate c-number stochastic equations whose variables correspond to quantum variables. In the derivation of the stochastic differential equations from the master equation there are at some

point, assumptions made about the validity of particular mathematical steps. It is to these assumptions that we must turn in order to locate the source of the problems with the representation. The numerical work of the previous sections indicated two features correlated with the failure of the positive P representation that require explanation—the appearance of power-law tails and the correlation with the earliest spike time. In this section we will outline two distinct procedures for deriving the stochastic differential equations and outline the likely causes of the numerical signatures.

A. Power-law tails

The appearance of a power-law tail in the averaged radial distribution of the P function almost certainly means that the boundary terms are significant and cannot be simply neglected. To see this we need to examine the convergence properties of the integral defining the positive P representation. The original definition [7] was purely formal in nature; namely, one defines nondiagonal projectors

$$\Lambda(\alpha,\alpha^+)=\frac{|\alpha\rangle\langle\alpha^{+*}|}{\langle\alpha^{+*}|\alpha\rangle} \tag{6.1}$$

and then a positive P function corresponding to a density operator ρ is one that satisfies

$$\rho=\int d^2\alpha\ d^2\alpha^+\Lambda(\alpha,\alpha^+)P(\alpha,\alpha^+). \tag{6.2}$$

How the convergence of the integral (6.2) is to be specified was not made clear in Ref. [7]. Since such issues are important, a more precise and rigorous definition is required; this was given by Gardiner [50] in terms of the quantum characteristic function, which is defined as

$$\chi(\lambda,\lambda^*)=\mathrm{Tr}\{\rho e^{\lambda a^\dagger}e^{-\lambda^* a}\}. \tag{6.3}$$

The quantum characteristic function characterizes the density operator completely [50]. It is clear that using Eq. (6.2) we can formally compute $\chi(\lambda,\lambda^*)$ and obtain a corresponding $\chi_P(\lambda,\lambda^*)$ defined in terms of $P(\alpha,\alpha^+)$:

$$\chi_P(\lambda,\lambda^*)=\int d^2\alpha\ d^2\alpha^+ e^{(\lambda\alpha^+-\lambda^*\alpha)}P(\alpha,\alpha^+). \tag{6.4}$$

This is the most convenient way of rigorously *defining* the positive P representation. Thus, we define a positive P function $P(\alpha,\alpha^+)$ by saying that if $\chi_P(\lambda,\lambda^*)$ as defined by Eq. (6.4) is such that $\chi_P(\lambda,\lambda^*)=\chi(\lambda,\lambda^*)$, then $P(\alpha,\alpha^+)$ is a positive P function corresponding to the density operator ρ.

Using the quantum characteristic function it was proved right at the beginning [7] that a positive P representation exists for any density operator, with

$$P(\alpha,\alpha^+)=\frac{1}{4\pi^2}\exp\left(\frac{-|\alpha-\alpha^+|^2}{4}\right)\left\langle\frac{\alpha+\alpha^+}{2}\middle|\rho\middle|\frac{\alpha+\alpha^+}{2}\right\rangle. \tag{6.5}$$

However, since the P representation is not unique, this is not necessarily the only P function for a given density operator. We need to establish conditions on a given $P(\alpha,\alpha^+)$ that ensure the existence of $\chi_P(\lambda,\lambda^*)$.

Questions of convergence are now reduced to the study of the integral (6.4). Notice that the Glauber-Sudarshan P representation would contain the exponential term $\exp\{\lambda\alpha^*-\lambda^*\alpha\}$, which has unit modulus, whereas in Eq. (6.4), the corresponding exponential can have an argument with arbitrarily large positive part. The definition of the order of integration can therefore be significant, since the mere fact that $P(\alpha,\alpha^+)$ can be normalized is *not* sufficient to guarantee the existence of $\chi_P(\lambda,\lambda^*)$. In Ref. [50] a condition for the existence of $\chi_P(\lambda,\lambda^*)$ for a given positive normalizable $P(\alpha,\alpha^+)$ is given. Namely, one writes

$$\alpha=re^{i\theta},\quad \alpha^+=r'e^{i\theta'},\quad \lambda=\mu e^{i\phi} \tag{6.6}$$

and carries out the θ,θ' integrations first as these clearly exist for any r,r' and λ.

Writing a Fourier series expansion

$$P(r,r',\theta,\theta')=\sum_{n=-\infty}^{\infty}\sum_{m=-\infty}^{\infty}c_{nm}(r,r')e^{in\theta}e^{im\theta'}. \tag{6.7}$$

It can be shown that a sufficient condition for the existence of $\chi_P(\lambda,\lambda^*)$ is that

$$|c_{-n,-m}(r,r')|r^{n+2+\epsilon}(r')^{m+2+\epsilon} \tag{6.8}$$

should be bounded for some nonzero ϵ, and all r,r'.

This condition, Eq. (6.8), which is rather strong, is already weaker than the condition for all moments of $P(\alpha,\alpha^+)$ to exist, which would require all $c_{n,m}$ to vanish faster than any power of r and r'.

A $P(\alpha,\alpha^+)$ that falls off as a Gaussian will not cause any problems and hence the simulations will be reliable. On the other hand, a $P(\alpha,\alpha^+)$ that falls off a power law comes dangerously close to condition (6.8). The degree of the power necessary so that $\chi_P(\lambda,\lambda^*)$ fails to exist is a problem that depends heavily on the particular situation under study. Certainly the simulations we have conducted suggest that for the averaged radial distribution in the variable $R=\sqrt{r^2+r'^2}$, a small power will inevitably lead to problems.

B. The earliest ''spike'' time

An alternative way of proceeding to derive the stochastic differential equations can be given in which no integration by parts is necessary, as follows. From the definition (6.3) an equation of motion for the quantum characteristic function $\chi(\lambda,\lambda^*,t)$ can be directly written using the correspondences

$$\rho a^\dagger\rightarrow\frac{\partial}{\partial\lambda}, \tag{6.9a}$$

$$a\rho\rightarrow-\frac{\partial}{\partial\lambda^*}, \tag{6.9b}$$

$$\rho a\rightarrow\left(\lambda-\frac{\partial}{\partial\lambda^*}\right), \tag{6.9c}$$

$$a^{\dagger}\rho \rightarrow \left(-\lambda^{*} + \frac{\partial}{\partial \lambda} \right), \tag{6.9d}$$

and no integration by parts is necessary, though it is necessary to take derivatives with respect to λ and λ^{*} inside the trace operation, which does require justification.

Similarly, we can write equivalences

$$\alpha P(\alpha,\alpha^{+}) \rightarrow -\frac{\partial}{\partial \lambda^{*}}, \tag{6.10a}$$

$$\alpha^{+} P(\alpha,\alpha^{+}) \rightarrow \frac{\partial}{\partial \lambda}, \tag{6.10b}$$

and similarly the derivation of these requires that derivatives with respect to λ and λ^{*} be taken inside the integral in the definition (6.4). This also requires justification.

The nature of the justification needed in the two cases is very different. In the first case, the quantum characteristic function can be written in the form

$$\frac{1}{\pi}\exp(|\lambda|^{2}) \int d^{2}\alpha \, \exp(\lambda\alpha^{*} - \lambda^{*}\alpha)\langle \alpha|\rho|\alpha\rangle. \tag{6.11}$$

The conditions under which the derivative may be taken inside the integral here are quite straightforward, since the integral is a two-dimensional Fourier transform of a positive normalizable function.

In the second case the integrand in Eq. (6.4) is not a Fourier transform, since the argument of the exponential is no longer purely imaginary, but may be any complex number. However, in both cases there will be some conditions under which the correspondences (6.9) and (6.10) are valid.

What can now be done is to take the solutions $\alpha(t)$, $\alpha^{+}(t)$, of the stochastic differential equation and define

$$\chi_{P} = \langle \exp[\lambda\alpha^{+}(t) - \lambda^{*}\alpha(t)] \rangle. \tag{6.12}$$

From this stochastic differential equation we find that $\chi_{P}(\lambda,\lambda^{*},t)$ obeys the same equation of motion as found for $\chi(\lambda,\lambda^{*},t)$ from the master equation.

The actual conditions for the validity of the correspondences (6.9) are dependent on the particular master equation being considered. Let us therefore illustrate with an example (consider the nonlinear absorber master equation treated in Sec. IV with $\gamma = 0$ and $\epsilon = 0$).

$$\frac{\partial \rho}{\partial t} = \frac{1}{2}(2a^{2}\rho a^{\dagger 2} - a^{\dagger 2}a^{2}\rho - \rho a^{\dagger 2}a^{2}). \tag{6.13}$$

Using Eq. (6.9) we find that the quantum characteristic function equation of motion is

$$\frac{\partial \chi}{\partial t} = -\frac{1}{2}\left[\left(\lambda^{*2} - 2\lambda^{*}\frac{\partial}{\partial \lambda} \right)\frac{\partial^{2}}{\partial \lambda^{*2}} + \left(\lambda^{2} - 2\lambda\frac{\partial}{\partial \lambda^{*}} \right)\frac{\partial^{2}}{\partial \lambda^{2}} \right]\chi. \tag{6.14}$$

The P-function characteristic function can be written directly in terms of the solutions $\alpha(t)$, $\alpha^{+}(t)$ as Eq. (6.12) and if we assume that $\alpha(t)$, $\alpha^{+}(t)$ obey Ito stochastic differential equations, we can expand to second order to get

$$\frac{\partial \chi_{P}}{\partial t} = \left\langle \exp[\lambda\alpha^{+}(t) - \lambda^{*}\alpha(t)] \left\{ \lambda \, d\alpha^{+}(t) + \frac{1}{2}\lambda^{2} d\alpha^{+}(t)^{2} - \lambda^{*} d\alpha(t) + \frac{1}{2}\lambda^{*2} d\alpha(t)^{2} - \lambda^{*}\lambda \, d\alpha^{+}(t) d\alpha(t) \right\} \right\rangle. \tag{6.15}$$

It is easy to see that the Ito stochastic differential equations [Eqs. (4.4) with $\gamma = \epsilon = 0$]

$$d\alpha = -\alpha^{2}\alpha^{+}dt + i\alpha dW_{1}(t), \tag{6.16a}$$

$$d\alpha^{+} = -\alpha^{+2}\alpha dt + i\alpha^{+} dW_{2}(t) \tag{6.16b}$$

will give exactly the same differential equation for $\chi_{P}(\lambda,\lambda^{*},t)$ as Eq. (6.14).

The manipulations involved in these two derivations are all formal, and take no account of the conditions required for their validity. The derivation of Eq. (6.14) is relatively easy to justify. A representation for the creation and destruction operators must be chosen, and in fact the easiest is to define all operators in terms of their action on the characteristic function itself, so that Eq. (6.14) is true by definition provided $\chi(\lambda,\lambda^{*},t)$ is itself always differentiable as many times as are required in the differential equation. It is clear that the condition for the existence of derivatives of order q for all λ including $\lambda = 0$ is that $|\alpha|^{q}\langle \alpha|\rho(t)|\alpha\rangle$ be a normalizable function. This is a condition with an easily understandable physical interpretation—for example, if we set $q = 2$, this is a condition on the finiteness of the mean energy, and higher values of q are related to limits on possible energy fluctuations. Thus, if the derivatives required for Eq. (6.14) fail to exist it is because something physically unusual is actually happening.

In contrast the derivation of Eq. (6.15) can fail for other reasons. In order for the ensemble averages in Eq. (6.15) to be valid requires that *all* the solutions of the differential equations (for all possible realizations of the noises) from the initial time up to and including the final time T.

1. General conditions

A set of stochastic differential equations

$$dX = f(t,X)dt + G(t,X)dW(t), \tag{6.17}$$

where X, $F(t,X)$, $dW(t)$ are vectors and $G(t,X)$ is a matrix, possesses solutions for all times in some finite interval and all initial conditions provided two conditions are satisfied.

(i) Generalized Lipshitz condition. For every $N > 0$, and all times in the desired interval, and all x,y such that $|x|,|y| \leq N$ there is a constant K_{N} such that

$$|f(x,t)-f(y,t)|+|G(t,x)-G(t,y)|\leqslant K_N|x-y|. \quad (6.18)$$

(ii) Restriction on growth. There exists a K such that for all t in the desired interval and all x

$$|f(x,t)|^2+|G(x,t)|^2\leqslant K(1+|x|^2). \quad (6.19)$$

It is clear that the stochastic differential equations (6.16) satisfy the generalized Lipshitz condition, but do not satisfy the growth condition. The typical behavior of such stochastic differential equations appears to be exactly that normally observed in positive P simulations: For a given initial condition the solution exists until a *random* time τ, at which stage it ''explodes to infinity.'' However, the random time τ need have no lower bound. For example, the stochastic differential equation

$$dy=y^3dt-y^2dW(t) \quad (6.20)$$

satisfies the generalized Lipshitz condition but not the growth condition, and has the explicit solution (found by substituting $y=1/x$)

$$x(t)=\frac{1}{x(0)^{-1}+W(t)-W(0)}. \quad (6.21)$$

Since $W(t)-W(0)$ is Gaussian with variance t, for any choice of $x(0)$ the denominator in Eq. (6.21) can vanish at any $t>0$.

2. The deterministic equation

The large α, α^+ behavior of the solutions of the stochastic differential equations (6.16) is dominated by the deterministic term, whose solutions are easy to find explicitly — it is sufficient to note that a solution for $\alpha^+\alpha$, when the noise terms are omitted is

$$\alpha^+\alpha=\frac{1}{A+2t}, \quad (6.22)$$

where $1/A$ is the initial value of $\alpha^+\alpha$. In the positive P representation this may be an arbitrary complex number, and in particular may be negative. But if A is negative the solution will cease to exist when $t=-A/2$. This kind of behavior is in general still present in the full equations including the noise terms—that is, if we start with an initial ensemble of points (α_i,α_i^+) contained within a bounded region of the phase space, then this kind of equation does not satisfy the conditions [51] necessary for the existence of a solution with a given initial condition in every finite interval $[0,T]$ after $t=0$.

Thus with any initial ensemble we may expect that there will be realizations of $W_1(t)$ and $W_2(t)$ that are such that the solution of the stochastic differential equations (6.16) with a particular initial condition chosen from the ensemble reach infinity in a *finite* time. Suppose that there is a lower bound t_e to all such times, and suppose the initial ensemble is such that $\int d^2\alpha d^2\alpha^+|\alpha|^q|\alpha^+|^{q'}P(\alpha,\alpha^+,0)$ exists for all q,q'. Then we conjecture that for $t<t_e$, (1) the characteristic function χ_P exists, (2) all λ,λ^* differentiations can be carried out under the integral signs, and (3) hence χ and χ_P obey the same partial differential equation (6.14) with the same initial condition and hence for $t<t_e$ we can conclude that $\chi_P=\chi$. This will mean that for $t<t_e$ a positive P-function simulation would give correct results. We cannot conclude that for $t\geqslant t_e$ the results will be wrong, but we have given ample evidence in the previous sections that this is very often the case. At $t=t_e$ the P function becomes unnormalizable, so that at that time the arguments that we can integrate by parts to get the P-function Fokker-Planck equation, and again to get the stochastic differential equations, also become invalid.

3. Topological barriers

There is currently just one known way to remove problems due to an unstable deterministic trajectory. This is for the distribution to always have a zero probability in the neighborhood of the trajectory. However, even when this is not exactly the case, the relevant probability may be an asymptotically vanishing quantity—allowing the boundary terms to become negligible in some limit. As was demonstrated in the preceding examples, the relevant asymptotic limit is typically that of small dimensionless nonlinearity. This limit turns out to have a great deal of significance, corresponding to the most common cases of physical interest.

The limit of small nonlinearity is the relevant limit as we have already seen in this paper, and we can express this in terms of a dimensionless coupling constant g, which is proportional to the ratio of nonlinearity to linearity (this the inverse of the quantity γ defined in Secs. I, IV, and V). In order for a true asymptotic limit to occur, it is essential that the probability for the dynamical system be in a neighborhood of an unstable deterministic trajectory, and approach zero faster than any power of g, as g approaches zero. If this is the case, then the size of the boundary term can scale in a nonanalytic way as $g\to 0$. An example of this would be if the probability was proportional to $e^{-|C/g|}$.

However, this is a common feature in equations of the Fokker-Planck type. In fact, it is the generic behavior for the diffusive penetration of a barrier, provided the diffusion (or noise) term scales proportional to g. Thus, if the singular trajectories become topologically isolated behind a barrier, the corresponding boundary corrections will be exponentially suppressed in the limit of small coupling constant. We emphasize here that the noise terms responsible for the complex trajectories are indeed proportional to the dimensionless coupling constant g of the nonlinear physical process. This provides an explanation for the numerically observed behavior, noted in the Introduction—in which large g values lead to boundary terms, which are dramatically reduced at small dimensionless couplings.

In summary, the main mechanism for the elimination of unwanted power-law tails and resulting boundary terms is a topological one. It is necessary for there to be a deterministic barrier between the initial values of the trajectories and the regions of singular initial conditions. The barrier is a region that divides the analytically continued complex phase space into (at least) two parts, with deterministic trajectories only traveling away from the unstable region. In these cases, no trajectory can cross from the initial region to the unstable region, without a stochastic driving force. Of course, transitions in the reverse direction must be deterministically allowed. If the noise vanishes on the barrier, the phase space is

dynamically separable, with the result that boundary terms can be exactly eliminated. If the noise is finite on the barrier, the boundary terms can still vanish asymptotically, as the dimensionless coupling parameter approaches zero. This latter case leads to a nonanalytic boundary term correction, which vanishes at small couplings.

VII. CONCLUSIONS

The conclusion that we reach is that for sufficiently nonlinear problems that involve small photon numbers the positive P simulation is only valid up to the earliest time at which a solution of the stochastic differential equations with initial values chosen from the given initial ensemble can reach infinity. At that time the P function becomes unnormalizable, and all arguments based on integration by parts and discarding surface terms at infinity also become questionable. However, the range of dynamical systems where the positive P representation has been demonstrated to fail is quite limited, and in any case these problems are better dealt with by other methods. We have found that directly simulating the master equation yields results far more easily than the positive P representation in these extreme parameter regimes. Furthermore, and more importantly, when the positive P simulations break down they do so in a predictable, and in an easily verifiable way.

We have shown, in summary, that this technique is frequently only asymptotically rather than exactly valid. Of course, the use of mathematical techniques that have asymptotic validity at small couplings is rather common in physics. For example, this is precisely the behavior of the Feynman diagram method in quantum field theory. Indeed, the Feynman diagram method and positive P calculations can be competing methods—for instance, the optical parametric oscillator near threshold has seen calculations both involving the Feynman diagram method [54,55] and positive P calculations [9,56–58].

We can give the following suggestions for the correct use of the positive P representation, noting that all problems (apart from computational problems) arise from the fact that the neglected boundary terms at infinity may not be negligible. Thus, when the positive P representation equations become inaccurate, they do so in a predictable way. Specifically, the presence of the following signatures indicate non-

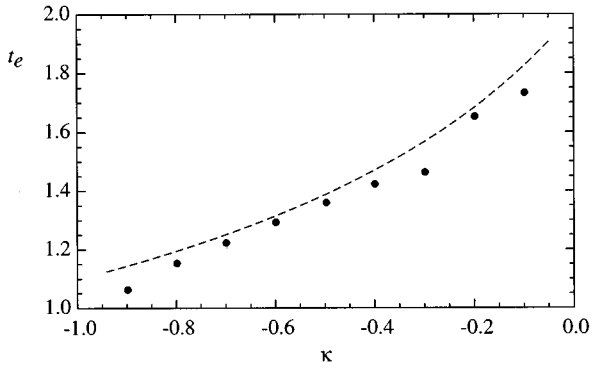

FIG. 21. Earliest occurring spike [trajectory reaching $\mathrm{Re}(N)\leqslant -40$] out of 1 000 spikes; the dots, plotted against the theoretical time t_e (dashed line), are from Eq. (A4).

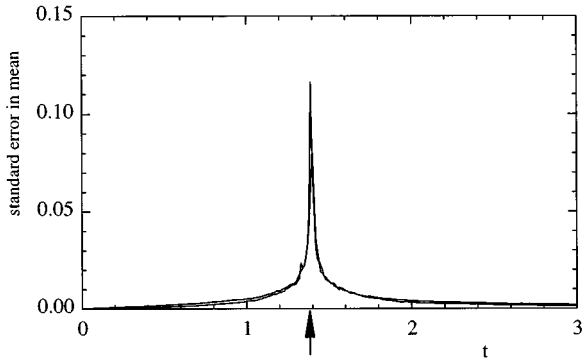

FIG. 22. Plot of the standard deviation of the mean, real, and imaginary parts, for an ensemble of 30 000 trajectories. All trajectories began at $N=-0.5$ and $\kappa=-0.5$. The result demonstrates a dramatic increase at the time t_e.

negligible boundary conditions. (1) The presence of ''spikes,'' typically large excursions into regions of phase space with $\mathrm{Re}(N)<0$, that are associated with singular deterministic trajectories. If spikes are seen, the solutions may not be reliable for all times after the earliest appearance of such spikes. It is not correct to simply discard such trajectories. (2) An increase in the statistical error of the distribution. This in essence corroborates the first signature. (3) The probability distribution develops power-law tails. This is the most quantitative indicator, but requires more numerical work to test. (4) The inclusion of more linear damping leads to the absence of the above indicators.

Provided sufficient care is taken to search for the numerical indicators above the positive P representation can be a useful and reliable tool.

ACKNOWLEDGMENTS

This project was supported by the New Zealand Foundation for Research, Science and Technology, under Contract No. UOW-306.

APPENDIX A: ANALYTIC EXAMPLE

This section will aim to illustrate that the behavior of the stochastic differential equations can flag a significant prob-

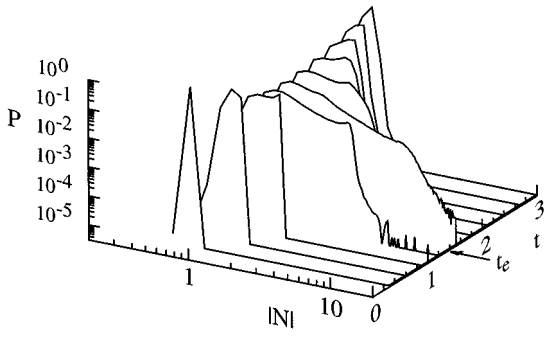

FIG. 23. Following the standard procedure presented elsewhere in the paper, 300 000 trajectories were binned according to their radii in phase space. Results show a power-law tail at the time t_e, using the parameter $\kappa=-0.5$ and the trajectories began at $N=-0.5$.

ability current at infinity that is, boundary term problems. The equations given do not correspond to a master equation, rather it is a modification of the noise term in Eq. (4.5) for the damped nonlinear absorber that allows an analytic solution to the resulting stochastic differential equations.

We modify Eq. (4.5) to

$$dN = -N(N+\kappa)dt + iN^2 dW, \tag{A1}$$

where the factor in front of the stochastic noise was again multiplied by N.

1. Analytical solution

Equation (A1) can be converted to the inverse variables $\nu = 1/N$; then splitting into real and imaginary parts we get

$$d\nu_r = (k\nu_r + 1)dt, \tag{A2a}$$

$$d\nu_i = k\nu_i dt - dW. \tag{A2b}$$

The real part has the solution

$$\nu_r(t) = \left(\nu_r^0 + \frac{1}{k}\right)e^{\kappa t} - \frac{1}{k} \tag{A3}$$

so that $\nu_r(t) = 0$ when

$$t_e = -\frac{1}{k}\ln(\kappa\nu_r^0 + 1). \tag{A4}$$

The imaginary part of Eqs. (A2) is equivalent to the Fokker-Planck equation

$$\frac{\partial P(\nu_i)}{\partial t} = \left[-\frac{\partial}{\partial \nu_i}(\kappa\nu_i) + \frac{1}{2}\frac{\partial^2}{\partial \nu_i^2}\right]P(\nu_i), \tag{A5}$$

which is an Ornstein-Uhlenbeck process and has the following solution [59], provided $t > 0$ and $P(\nu_i, t|0,0) = \delta(\nu_i)$:

$$P(\nu_i) = [\pi b(t)]^{-1/2} e^{-\nu_i^2/b(t)}, \tag{A6a}$$

$$b(t) = (e^{2\kappa t} - 1)/\kappa. \tag{A6b}$$

Now, combining the real and imaginary parts we have

$$P(\nu_r, \nu_i, t|\nu_r^0, 0, 0) = [\pi b(t)]^{-1/2}\delta(\nu_r - \nu_r(t))e^{-\nu_i^2/b(t)}, \tag{A7a}$$

$$\nu_r(t) = (\nu_r^0 + \kappa^{-1})e^{\kappa t} - \kappa^{-1}. \tag{A7b}$$

Then, transform P back to the original variables but in polar coordinates $N = re^{i\theta}$:

$$P(r,\theta,t|\nu_r^0,0,0) = \frac{\delta(\cos\theta - \nu_r(t)r)}{r^3\sqrt{\pi b(t)}}e^{-\sin^2\theta/[r^2 b(t)]}, \tag{A8}$$

and finally, integrate out the θ variable:

$$P(r,t|\nu_r^0,0) = \frac{2\Delta[1-\nu_r^2(t)r^2]}{r^3\sqrt{\pi b(t)}}e^{-[1-\nu_r^2(t)r^2]/[r^2 b(t)]}, \tag{A9}$$

where $\Delta = 1$ if $a \geq 0$, and 0 if $a \leq 0$.

It is easy to see that $P(r,t|\nu_r^0,0)$ is strictly bounded within a radius $r \leq |\nu_r(t)|^{-1}$ and that this will become infinite at a time t_e given by Eq. (A4).

If this were an example derived from an actual master equation there would be no doubt as to the validity of neglecting the boundary terms before the time t_e. After the time t_e we cannot have such confidence, since there is obviously a nonzero current at infinity.

2. Numerical signatures

Given this example is analytically tractable, it serves to test the numerical signatures. That is, we should be able to predict the time t_e based on purely numerical work. With this done, we can have confidence in predicting a similar time at which the positive P representation is expected to fail for examples that are not so easily analyzed.

a. Presence of spikes

The easiest indicator to monitor is the presence of spikes in the simulation. Often these will show their presence in the averages obtained, though we recommend actively searching for them by identifying trajectories that make an excursion beyond some suitable boundary.

As depicted in Fig. 21, we collected 1000 spikes [defined as trajectories reaching $\mathrm{Re}(N) \leq -40$]. The earliest of these spikes to occur forms a good indicator of the time t_e calculated in Eq. (A4).

b. Increase in the statistical error

As is clearly demonstrated in Fig. 22 the onset of spiking is accompanied by a large increase in the statistical error of the distribution. The initial condition is unphysical, but this is a test case with no physical significance; the initial condition was chosen to give a reasonable value of t_e. The purpose is to predict the time at which the boundary terms will become a problem.

c. Development of a power-law tail

Finally, as seen in Fig. 23, the tail of the distribution begins to fall off as a power law at the time t_e, giving clear evidence of boundary term problems. It is clear then that the numerical signatures can reliably predict the time at which boundary terms will cause problems (that is, the time t_e). The presence of these signatures casts doubt on the validity of the solution from the time of their occurrence onward.

APPENDIX B: THE LASER EQUATIONS NEAR THRESHOLD

Equations (3.6) for the laser can be further scaled by setting $d\tau = d\tau'/\epsilon$ and $\tilde{\alpha} = \sqrt{\epsilon}\tilde{\alpha}'$ giving the Ito stochastic equations

$$d\tilde{\alpha}' = (\tilde{\alpha}' - \tilde{\alpha}'^{+}\tilde{\alpha}'^{2})d\tau' + \sqrt{\tilde{Q}/\epsilon^2}dW', \tag{B1a}$$

$$d\tilde{\alpha}'^{+} = (\tilde{\alpha}'^{+} - \tilde{\alpha}'^{+2}\tilde{\alpha}')d\tau' + \sqrt{\tilde{Q}/\epsilon^2}dW'^{*} \tag{B1b}$$

and an initial variance of $(\epsilon\mathcal{N})^{-2} = C/n_0(C-1)$, which near threshold becomes very large. However, the noise parameter is now

$$\left(\frac{\tilde{Q}}{\epsilon^2}\right)^{1/2}=\left(\frac{[\kappa n+\tilde{g}^2(1+\overline{d})/2\overline{\gamma}]C}{\kappa n_0(C-1)^2}\right)^{1/2}, \qquad \text{(B2)}$$

which also becomes very large near threshold, and this effect was not taken into account by Schack and Schenzle.

[1] R. J. Glauber, Phys. Rev. **131**, 2766 (1963).
[2] E. C. G. Sudarshan, Phys. Rev. Lett. **10**, 277 (1963).
[3] E. P. Wigner, Phys. Rev. **40**, 749 (1932).
[4] K. Husimi, Proc. Phys. Math. Soc. Jpn. **22**, 264 (1940).
[5] K. E. Cahill and R. J. Glauber, Phys. Rev. **177**, 1882 (1969).
[6] P. D. Drummond, Phys. Rev. A **33**, 4462 (1986).
[7] P. D. Drummond and C. W. Gardiner, J. Phys. A **13**, 2353 (1980).
[8] J. R. Klauder and E. C. G. Sudarshan, *Fundamentals of Quantum Optics* (Benjamin, New York, 1970).
[9] P. Kinsler and P. D. Drummond, Phys. Rev. A **43**, 6194 (1991).
[10] P. Kinsler and P. D. Drummond, Phys. Rev. A **44**, 7848 (1991).
[11] P. Kinsler, M. Fernée, and P. D. Drummond, Phys. Rev. A **48**, 3310 (1993).
[12] J. R. Klauder, S. L. McCall, and B. Yurke, Phys. Rev. A **33**, 3204 (1986).
[13] V. Perinova, J. Krepelka, and J. Perina, Opt. Acta **33**, 1263 (1986).
[14] M. D. Reid and D. F. Walls, Phys. Rev. A **34**, 4929 (1986).
[15] H. J. Carmichael, Phys. Rev. A **33**, 3262 (1986).
[16] P. D. Drummond and S. J. Carter, J. Opt. Soc. Am. B **4**, 1565 (1987).
[17] M. Xiao, H. J. Kimble, and H. J. Carmichael, Phys. Rev. A **35**, 3832 (1987).
[18] P. D. Drummond and M. D. Reid, Phys. Rev. A **37**, 1806 (1988).
[19] F. A. M. de-Olivera and P. L. Knight, Phys. Rev. A **39**, 3417 (1989).
[20] B. Huttner and Y. Ben-Aryeh, Phys. Rev. A **40**, 2479 (1989).
[21] M. J. Collett and D. F. Walls, Phys. Rev. Lett. **61**, 2442 (1988).
[22] C. M. Savage and T. C. Ralph, Phys. Rev. A **46**, 2803 (1992).
[23] W. Kaige, Phys. Rev. A **37**, 4785 (1988).
[24] A. Eschmann and M. D. Reid, Phys. Rev. A **49**, 2881 (1994).
[25] T. A. B. Kennedy and D. F. Walls, Phys. Rev. A **37**, 152 (1988).
[26] W. J. Munro and M. D. Reid, Phys. Rev. A **47**, 4412 (1993).
[27] Y. Qu, M. Xiao, G. S. Holliday, S. Singh, and H. J. Kimble, Phys. Rev. A **45**, 4932 (1992).
[28] M. Wolinsky and H. J. Carmichael, Phys. Rev. Lett. **60**, 1836 (1988).
[29] M. D. Reid and B. Yurke, Phys. Rev. A **46**, 4131 (1992).
[30] M. D. Reid and L. Krippner, Phys. Rev. A **47**, 552 (1993).
[31] R. Vyas and S. Singh, Phys. Rev. Lett. **74**, 2208 (1995).
[32] S. J. Carter, P. D. Drummond, M. D. Reid, and R. M. Shelby, Phys. Rev. Lett. **58**, 1841 (1987).
[33] M. G. Raymer, P. D. Drummond, and S. J. Carter, Opt. Lett. **16**, 1189 (1991).
[34] P. D. Drummond and M. G. Raymer, Phys. Rev. A **44**, 2072 (1991).
[35] A. Eschmann and C. W. Gardiner, Phys. Rev. A **49**, 2907 (1994).
[36] G. S. Agarwal and S. Chaturvedi, Phys. Rev. A **49**, R665 (1994).
[37] S. J. Carter and P. D. Drummond, Phys. Rev. Lett. **67**, 3757 (1991).
[38] N. Lu, S.-Y. Zhu, and G. S. Agarwal, Phys. Rev. A **40**, 258 (1989).
[39] M. L. Steyn, M.Sc. thesis, University of Waikato, 1979 (unpublished).
[40] M. Dörfle and A. Schenzle, Z. Phys. B **65**, 113 (1986).
[41] S. Sarkar, J. S. Satchell, and H. J. Carmichael, J. Phys. A **19**, 2765 (1986).
[42] J. S. Satchell, and S. Sarkar, J. Phys. A **19**, 2737 (1986).
[43] A. M. Smith and C. W. Gardiner, Phys. Rev. A **1**, 3511 (1989).
[44] I. J. D. Craig and K. J. McNeil, Phys. Rev. A **39**, 6267 (1989).
[45] K. J. McNeil and I. J. D. Craig, Phys. Rev. A **41**, 4009 (1990).
[46] R. Schack and A. Schenzle, Phys. Rev. A **44**, 682 (1991).
[47] C. W. Gardiner and A. S. Parkins, Phys. Rev. A **50**, 1792 (1994).
[48] H. J. Carmichael, J. S. Satchell, and S. Sarkar, Phys. Rev. A **34**, 3166 (1986).
[49] S. Sarkar and J. S. Satchell, J. Phys. A **20**, 2147 (1987).
[50] C. W. Gardiner, *Quantum Noise* (Springer-Verlag, Heidelberg, 1991).
[51] C. W. Gardiner, *Handbook of Stochastic Methods* (Springer-Verlag, Heidelberg, 1983).
[52] C. W. Gardiner, A. Gilchrist, and P. D. Drummond, in *Using the Positive P Representation*, edited by F. Ehlotzky, Lecture Notes in Physics, Vol. 420 (Springer-Verlag, Berlin, 1993), p. 239.
[53] Ts. Gantsog and R. Tanaś, Phys. Rev. A **44**, 2086 (1991).
[54] C. J. Mertens, T. A. B. Kennedy, and S. Swain, Phys. Rev. A **48**, 2374 (1993).
[55] L. I. Plimak and D. F. Walls, Phys. Rev. A **50**, 2627 (1994).
[56] P. D. Drummond, K. J. McNeil, and D. F. Walls, Opt. Acta **28**, 211 (1981).
[57] P. D. Drummond and P. Kinsler, Quantum Semiclass. Opt. **7**, 727 (1995).
[58] S. Chaturvedi and P. D. Drummond, Phys. Rev. A **55**, 912 (1997).
[59] H. Risken, *The Fokker-Plank Equation* (Springer-Verlag, Berlin, 1984).